Cloud Responses to Abrupt Solar and CO_2 Forcing Part I: Temperature Mediated Cloud Feedbacks

Enter authors here: T. Aerenson[1] and R. Marchand[1]

[1]University of Washington Department of Atmospheric Sciences.

Corresponding author: Travis Aerenson (aerenson@uw.edu)

Key Points:

- The temperature mediated cloud changes and feedbacks incurred by changes in solar and CO_2 forcing are similar.
- Optical depth changes at high latitudes produce substantial differences in cloud feedbacks in cooling and warming experiments.
- Likewise, tropical circulations respond differently in models to cooling and warming, with a stronger change in the Walker circulation in warming experiments.

Abstract

The third phase of the Cloud Feedback Model Intercomparison Project requested that modeling centers perform a pair of simulations where the climate system is subjected to an abrupt change of the solar constant by +/- 4%. The forcing is designed to loosely match the amount of radiative forcing incurred by quadrupling atmospheric CO_2 concentrations. Using these simulations, we examine how clouds respond to changes in solar forcing and act as a feedback on global surface temperature. Specifically, in this paper, we study the temperature mediated cloud changes that occur following an abrupt increase and decrease of the solar constant and compare with temperature mediated cloud changes that occur following quadrupling and halving of CO_2. We seek to answer two primary questions: 1) How do cloud feedbacks differ in response to abrupt changes in CO_2 and solar forcing? And 2) Are there symmetrical (equal and opposite) cloud feedbacks to an increase and a decrease in solar forcing?

We find that temperature mediated cloud changes are similar from increasing solar and CO_2 forcing, with the only robust difference being that there is a larger reduction of low cloud amount following solar forcing; and we find that cloud responses to warming and cooling are not symmetric, due primarily to non-linearity introduced by phase changes in mid-to-high latitude low clouds, and sea ice loss/formation.

Plain Language Summary

As the global mean temperature changes, there are changes in cloud amount, location, and thickness, which can all impact the radiative balance of the Earth. Cloud changes driven directly by global temperature change are called temperature mediated cloud feedbacks. In this paper we study the temperature mediated cloud feedbacks that occur in model simulations where the amount of sunlight incident upon the Earth is increased or decreased abruptly, and then held constant for 150 years. We compare the cloud changes in these experiments with experiments where the CO_2 concentration is similarly increased or decreased abruptly and held constant for 150 years. In doing so we find that the temperature mediated cloud feedbacks following abrupt changes in solar radiation are characteristically similar to those occurring following CO_2 increase. There are however substantial differences in the temperature mediated cloud feedbacks that occur while the climate is warming vs cooling.

1. <u>Introduction</u>

As the climate warms due to the radiative forcing created by increasing CO_2 and other heat trapping gasses, one anticipates that many aspects of the climate system will experience change. Some of these changes will further impact the Earth radiation balance, creating feedback loops. Radiative feedbacks related to changes in cloud properties and cloud amount have been identified as the largest source of uncertainty (spread) in projections of future climate (e.g. Sherwood et al., 2020; Zelinka et al., 2020). To better understand cloud responses to forcing, in this paper we examine cloud feedbacks which occur following an abrupt increase and decrease in solar radiation and contrast these solar-driven changes with those caused by abrupt changes in CO_2 concentrations in several climate models. We do this because (as will be shown) both differences and similarities in the responses between these two types of forcing provides insight into the mechanisms that drive the changes, and in doing so we hope to better pinpoint the expected cloud changes that will occur in response to ongoing changes in actual emissions of heat trapping gasses.

Radiative feedbacks (including cloud feedbacks) are often quantified in climate model simulations by the relationship between the top-of-atmosphere radiative flux and global-mean surface temperature change (compared to a simulation of the pre-industrial climate), and this relationship is often approximated as a linear response (Gregory et al., 2004). The linear model separates the total change into a temperature mediated change (the cloud change per degree of global mean temperature anomaly) and an adjustment that occurs directly due to the forcing agent (in our case from changes in insolation or atmospheric CO_2 concentration). In this paper we focus on the temperature mediated component of the cloud response to solar and CO_2 forcing, while in a companion paper (Part II, Aerenson et al., 2023), we focus on the cloud adjustments.

Often the temperature mediated changes in top-of-atmosphere radiative flux are simply called radiative feedbacks, or when they are due to clouds, simply cloud feedbacks. Cloud feedbacks constitute the largest source of uncertainty in projections of future climate. Naturally, cloud feedbacks that occur from CO_2 increase have become a widely studied topic. (e.g. Andrews & Ringer, 2014; Dufresne & Bony, 2008; Sherwood et al., 2020; Taylor et al., 2007; Zelinka et al., 2020). Here, we analyze cloud feedbacks in model simulations produced as a part of the third phase of the Cloud Feedback Model Intercomparison Project (CFMIP3; Webb et al., 2017) which is a part of the sixth phase of the Coupled Model Intercomparison Project (CMIP6). Specifically, in CFMIP3 a pair of model simulations were performed in fully coupled climate models initialized from the pre-industrial climate, and then perturbed by suddenly increasing or decreasing the insolation by 4% (hereafter solp4p and solm4p respectively). We compare and contrast these two abrupt-solar experiments with simulations in which there is an abrupt quadrupling of the CO_2 concentration (hereafter 4xCO2) and halving of CO_2 (hereafter 0p5xCO2) that were also produced as a part of the CMIP6 experiments (Eyring et al., 2016). An increase of the solar constant by 4% is designed to (loosely) match the radiative forcing of a quadrupling of atmospheric CO_2, and as we will see, the experiments do produce a similar change in the mean global temperature. In contrast, a reduction of solar constant by 4% does not match closely with the radiative forcing from 0p5xCO2, and again, as we will see, there are differences in the feedbacks between the solm4p and 0p5xCO2 related to the amplitude of the forcing.

Through this analysis, we seek to answer two primary questions: 1) How do cloud feedbacks differ in response to abrupt changes in CO_2 and solar forcing? And 2) Are there symmetrical (equal and opposite) cloud feedbacks to an increase and a decrease of radiative forcing? Additionally, we aim to examine the physical mechanisms responsible for the temperature mediated cloud changes in the four model experiments.

For obvious reasons, cloud feedbacks resulting from CO_2 increase have been more widely studies than those from solar forcing (e.g. Andrews & Ringer, 2014; Dufresne & Bony, 2008; Sherwood et al., 2020; Taylor et al., 2007; Zelinka et al., 2020). Recently, Kaur et al. (2023) performed coupled model experiments of an abrupt doubling of CO_2 and a 2% increase of the solar constant with a single model. They found differences in the temperature mediated feedbacks caused by the differences in geographic distributions of each forcing. CO_2 increase has an instantaneous radiative forcing that is homogeneously distributed across the globe and is equal during all seasons. Solar forcing differs in that it is strongest in regions with more incident sunlight, so the forcing is greatest in the tropics and during the summer season. This causes a difference in the warming patterns from solar and CO_2 forcing, where the tropics are warmer, and the poles are cooler following a 2% increase in solar forcing compared with a doubling of CO_2. They also find differences in the cloud feedbacks in their experiments, such as finding greater decrease of high cloud and lesser decrease in low clouds in the solar forcing experiment than CO_2. However, this study was based on the output of a single climate model, and cloud feedbacks have notoriously large inter-model spread (Sherwood et al., 2020; Soden & Held, 2006; Zelinka et al., 2020), as such, our study expands upon this analysis by focusing more narrowly on the cloud changes (and their causes) from solar and CO_2 forcing in several models.

Comparing solar and CO_2 forcing is also relevant for understanding how we expect the climate to respond to aerosol forcing, as both changing the solar constant and aerosol forcing change the downwelling shortwave radiation. Salvi et al. (2022) used model simulations forced with historical greenhouse gas, and historical aerosol forcing separately to compare the contributions of longwave (greenhouse gas) and shortwave (aerosol) forcing in model simulations of the historical climate record. In doing so, they found that historical aerosol forcing (which is most concentrated in the midlatitudes) has a greater impact on low clouds than CO_2 forcing (which is globally uniform). They also find that the different geographic distributions of forcing is the most important determinant of cloud feedbacks from historical aerosol and greenhouse gas emissions. Hence, the results of Salvi et al. (2022) suggests that in our comparison of solar and CO_2 forcing, we should expect a greater change in midlatitude low clouds from CO_2 forcing (which is globally uniform), than solar forcing (which is greatest in the tropics).

A broadly similar result was found by Rose et al. (2014), who used climate model simulations forced by ocean heat uptake in the tropics and midlatitudes (as well as 4xCO2) to determine how the location of forcing impacts climate feedbacks. They found that forcing applied in the extratropics yields more positive cloud feedbacks than globally uniform forcing, and globally uniform forcing yields more positive cloud feedbacks than forcing applied to the tropics. This emphasizes the result that cloud feedbacks are more positive when the forcing is concentrated in the extratropics, which suggests that we should expect more positive feedbacks from 4xCO2 than solp4p. However, as we will see, this is opposite of what we find in Section 3.2.

The second question, on the differences between cooling and warming the climate has received far less attention than characterizing the effects of warming the climate, and understanding the climate's response to abrupt negative forcing is an essential step to understanding more realistic forcing that acts to cool the climate, such as volcanic aerosol forcing, and various methods of geoengineering that aim to reduce the amount of sunlight absorbed by the Earth through techniques such as stratospheric aerosol injection or marine cloud brightening (e.g. Hulme, 2012; Keith et al., 2016; Niemeier et al., 2013; Shepard et al., 2009).

Chalmers et al., (2022) studied the climate's response to abruptly increasing and decreasing CO_2 and performed additional cloud-locking experiments to isolate the effects of the cloud changes from the non-cloud climate changes. They found that patterns in Tropical Pacific sea-surface temperature changes differ notably between increasing and decreasing CO_2 (warming and cooling) experiments, and have a large impact on atmospheric circulation, and teleconnections across the globe. They also found that disabling cloud feedbacks vastly reduces the pattern difference between warming and cooling (meaning that cloud feedbacks play an important role in changing the global temperature pattern). Additionally, they found significant differences in the high latitude oceans, where there is liquification and glaciation of mixed-phase clouds from warming and cooling respectively occurring at different latitudes, as well as sea-ice reduction and growth in the warming and cooling occurring at different latitudes which is likewise amplified by cloud feedbacks.

For the temperature mediated response to cooling and warming to be symmetrical (equal and opposite) then it would be the case that the same linear model is effective for cloud changes over the range of climate states from a 4% reduction of the solar constant to a 4% increase of the solar constant. Studies by both Bloch-Johnson et al. (2021) and Zhu & Poulsen (2020) on the linearity of feedbacks find that cloud feedbacks change depending on the amount of abrupt forcing due to the mixed-phase cloud feedback and sea-ice-related feedbacks because both of these feedbacks occur at different latitudes depending on the global mean temperature change (Bloch-Johnson et al., 2021). Zhu & Poulsen (2020) also identified a nonlinear change in shortwave cloud feedbacks at low latitudes, due to the nonlinear change in the moisture gradient between the boundary layer and free troposphere that enhances low cloud thinning through dry air entrainment from the free troposphere. As such, we anticipate that the temperature mediated cloud changes may differ from cooling and warming, especially in regions where there are changes in sea-ice, mixed-phase clouds, and low-latitude low clouds.

This paper is organized as follows, the model output and method for calculating the temperature mediated cloud changes and the associated radiative effect are summarized in Section 2. Results are presented in Section 3 and are split into six subsections. The first subsection examines the cloud responses in the solp4p, 4xCO2, solm4p, and 0p5xCO2 experiments. The second subsection examines the radiative effect of the cloud changes, and the remaining four subsections are dedicated to exploring the physical mechanisms responsible for the cloud changes. This is followed by additional discussion and conclusions in Sections 4 and 5 respectively.

2. Data and Methods

2.1 Methods and Theory

When an abrupt forcing is imposed on the climate, the cloud changes are often decomposed into two components: those driven by changes in global mean surface temperature (which are called temperature mediated change) and those that are independent of the global mean surface temperature (which are called the adjustments), as described by Equation 1, where $C(\theta, \phi, t)$ represents the cloud amount anomaly at a given latitude, longitude, and time in the simulation, $A(\theta, \phi)$ is the adjustment to the forcing change at a certain latitude and longitude, $\Delta T(t)$ is the global mean surface temperature anomaly at a given time, $M\big(\theta, \phi, T(t)\big)\Delta T(t)$ is the temperature mediated component of the cloud anomaly, and ε represents internal variability which causes cloud changes which are due to neither the global mean temperature change or adjustments. In this paper, we are concerned with calculating the adjustment term $A(\theta, \phi)$.

$$C(\theta, \phi, t) = A(\theta, \phi) + M\big(\theta, \phi, T(t)\big)\Delta T(t) + \varepsilon \qquad (1)$$

Often the temperature mediated changes are approximated by a linear relationship to global mean surface temperature, such that M is a constant in temperature (and time) $M\big(\theta, \phi, T(t)\big) \approx M(\theta, \phi)$ following the framework of Gregory et al. (2004). The temperature mediated component of cloud changes ($M(\theta, \phi)$) is calculated via a least-squares linear regression of annual mean changes in cloud amount (often for a specific cloud type or category, and at a specific location or globally averaged) onto the annual and global mean surface temperature anomaly, using years 10 to 150 following the abrupt forcing. The first 9 years are excluded because shortly following the forcing the linear model does not fit well to the simulated data due to a combination of the internal variability, and the inherently non-linear nature of the climate's response to abrupt forcing (e.g. Andrews & Ringer, 2014; Armour et al., 2013; Williams et al., 2008). By using 140-year regressions and excluding the first 9 years of simulation we expect that internal variability has little contribution to the temperature mediated cloud changes we calculate. As such Equation 1 is simply reduced to a linear model where cloud changes depend on the adjustment to forcing (A), surface temperature change (ΔT), and the temperature mediated term (M).

$$C(\theta, \phi, t) = A(\theta, \phi) + M(\theta, \phi)\Delta T(t) \qquad (2)$$

In this paper, we focus on the temperature mediated term calculated following abrupt solar and CO_2 forcing, as well as the temperature mediated response to warming and cooling. In Part II, we focus on the cloud adjustments to solar and CO_2 forcing.

To perform a comparison of cloud changes across models this study also makes extensive use of the International Satellite Cloud Climatology Project (ISCCP) satellite simulator embedded into the climate models. Specifically, the ISCCP simulator produces cloud-top-pressure (CTP) and optical depth joint histograms of cloud occurrence that are directly comparable across models, and consistent with the radiation scheme within each model (Bodas-Salcedo et al., 2011).

Zelinka et al. (2012a) have created cloud radiative kernels to compute longwave (hereafter LW) and shortwave (hereafter SW) fluxes from the ISCCP histograms. Using the radiative kernels, Zelinka et al. (2013) have examined cloud adjustments and temperature mediated responses to 4xCO2 simulations from a collection of CMIP5 models. The findings from Zelinka et al. (2013) include a temperature mediated increase in cloud-top-height for high-altitude clouds at nearly all locations that leads to a strong LW temperature mediated feedback, decrease in low-altitude clouds equatorward of 60° latitude causing a positive SW feedback, and thickening of high latitude low-altitude cloud optical depth leading to negative SW cloud feedback. Here we undertake a similar analysis but applied to the solar forcing experiments in addition to the 4xCO2 and 0p5xCO2 experiments performed by the current generation of climate models used in CMIP6. In order to understand the radiative impact that temperature mediated changes of cloud cover fraction (CF), cloud-top-pressure (CTP), and cloud optical depth (τ) have on top-of-atmosphere radiation balance (feedbacks), we perform a decomposition of the kernel-derived radiative effect into the radiative anomalies caused by each type of cloud change (as well as a small residual), following the method of Zelinka et al. (2012b & 2013).

2.2 Model Experiments

In total five modeling centers performed the solp4p experiment, and four performed the solm4p. The models are listed in **Table 1**, along with the experiments we make use of here, and a primary citation for each model. CESM2 did perform all the simulations, however there is no ISCCP simulator output for the 4xCO2 simulation, so CESM2 is excluded from the portion of the analysis where the ISCCP simulator output is compared between the solar and CO_2 forced experiments. All model simulation output is publicly available for download on the Earth System Grid Federation CMIP6 database (https://esgf-node.llnl.gov/search/cmip6/).

Model	Simulations used	Reference
CESM2	PiControl (no ISCCP simulator) Abrupt-solp4p Abrupt-solm4p Abrupt-4xCO2 (no ISCCP simulator)	Danabasoglu et al. (2020)

	Abrupt-0p5xCO2	
IPSL-CM6A-LR	PiControl Abrupt-solp4p Abrupt-solm4p Abrupt-4xCO2 Abrupt-0p5xCO2	Boucher et al. (2020)
CanESM5	PiControl Abrupt-solp4p Abrupt-solm4p Abrupt-4xCO2 Abrupt-0p5xCO2	Swart et al. (2019)
HadGEM3-GC31-LL	PiControl Abrupt-solp4p Abrupt-4xCO2 Abrupt-0p5xCO2	Roberts et al. (2019)
MRI-ESM2-0	PiControl Abrupt-solp4p Abrupt-solm4p Abrupt-4xCO2 Abrupt-0p5xCO2	Yukimoto et al. (2019)

Table 1 *Summary of models and data used in this analysis along with primary citations for each model. CESM2 did not produce ISCCP simulator output from the 4xCO2 and piControl experiments, so it is generally excluded from the analysis of cloud attributes, but the model is used to characterize other physical responses to the forcing.*

3. <u>Results</u>

In this section we present the results showing the temperature mediated cloud changes in model simulations with solar and CO_2 forcing and examine the cloud radiative effect the temperature mediated cloud changes have on top-of-atmosphere radiation using cloud radiative kernels. In Section 4 we discuss the physical mechanisms that likely contribute to the cloud changes, and as a prelude to that discussion we include in this section an examination of changes in atmospheric circulations and several other atmosphere and surface variables.

<u>3.1 Temperature Mediated Response in Cloud Properties to Solar and CO_2 Forcing</u>

The primary focus of this section is to examine how cloud properties respond to global temperature change that is forced by increases and decreases of the solar constant and CO_2 concentration. **Figure 1** shows the change in global total cloud amount (summed over all optical depth and CTP bins of the ISCCP simulator) that occurs in each simulation plotted against the global mean temperature anomaly from the simulation of the pre-industrial climate.

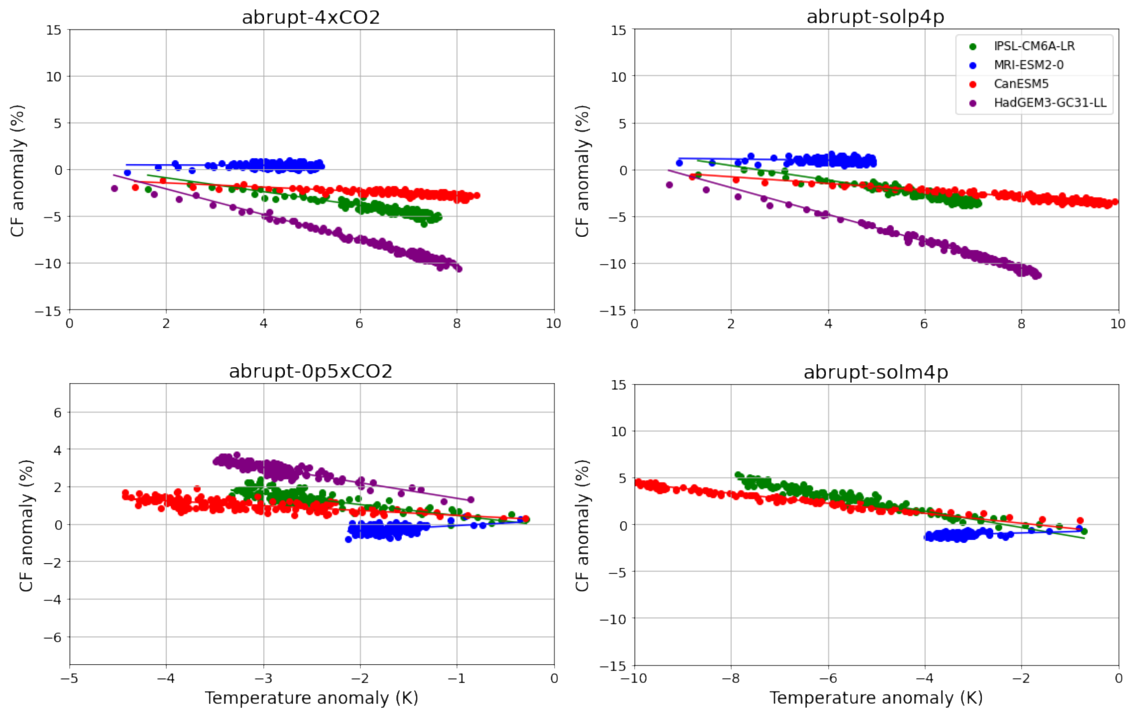

Figure 1 *Area weighted global mean cloud fraction anomaly (as seen by ISCCP simulator) plotted against global mean temperature change. Note that the scale is halved for the 0p5xCO2 simulation because the temperature change is smaller than in the other experiments.*

Colors denote the individual models. The temperature mediated change in global total cloud amount (for each model) is given by the slope of the fitted line. In the 4xCO2 and solp4p simulations there is a reduction of cloudiness as the climate warms in all but the MRI-ESM2-0 simulations (which shows near-zero temperature mediated change). The slopes and intercepts of each model in **Figure 1** (and the multi-model mean) are listed in **Tables 2 and 3**. While there is substantial spread in the response of different models, the temperature mediated response for each individual model (in the global mean) is quite similar in both the 4xCO2 and solp4p experiments. However, the solp4p temperature mediated change in cloud amount is persistently slightly more negative than the 4xCO2.

Model	**Total Cloud Amount Temperature Mediated Change (%/K)**			
Experiment	4xCO2	0p5xCO2	Solp4p	Solm4p
IPSL-CM6A-LR	-0.74	-0.59	-0.78	-0.88
MRI-ESM2-0	-0.02	0.27	-0.06	0.14
CanESM5	-0.22	-0.26	-0.36	-0.53
HadGEM3-GC31-LL	-1.36	-0.83	-1.43	N/A
MM Mean	-0.59	-0.35	-0.66	-0.43

Table 2 *Temperature mediated changes of total cloud amount for each model simulation.*

Model	**Total Cloud Amount Intercept (%)**			
Experiment	4xCO2	0p5xCO2	Solp4p	Solm4p
IPSL-CM6A-LR	0.55	-0.16	1.94	-2.11
MRI-ESM2-0	0.47	0.17	1.21	-0.65
CanESM5	-1.03	0.18	-0.10	-0.95
HadGEM3-GC31-LL	0.62	0.52	0.90	N/A
MM Mean	0.16	0.18	0.99	-1.24

Table 3 *Intercept of linear fit to the data shown in* ***Figure 1****.*

In the solm4p there is one fewer model than the other experiments. Yet even on a model-to-model basis, it is apparent that there are greater differences in the magnitude of the global mean temperature mediated response between cooling and warming than between solar or CO_2 forcing. For example, in CanESM5, the global mean temperature mediated cloud change in solm4p is more than double that of either 4xCO2 or solp4p, and in MRI-ESM2, the temperature mediated cloud change is of opposite sign in solm4p and 0p5xCO2 from the solp4p and 4xCO2 experiments. The 0p5xCO2 also exhibits differences from the solm4p (which may be due in part to the smaller forcing that halving CO_2 imposes on the climate as compared with a 4% reduction of the solar constant).

Across all four experiments HadGEM3-GC31-LL produces the most negative temperature mediated cloud response, IPSL-CM6A-LR has the second most negative, followed by CanESM5, and MRI-ESM2-0 either has the least negative temperature mediated cloud change (in the case of solp4p and 4xCO2) or a positive temperature mediated change (in the case of solm4p and 0p5xCO2).

The geographic distributions of the temperature mediated cloud responses are shown in **Figure 2** for the 4xCO2 and solp4p experiments. In this figure, the temperature mediated response of cloud fraction is calculated at each grid cell, for nine pressure and optical depth categories using the ISCCP simulator. Specifically the cloud optical depth is broken into three ranges: optically thin ($\tau \leq 3.6$), medium ($3.6 < \tau \leq 23$), and thick ($\tau > 23$) clouds, and the CTP is likewise broken into three CTP ranges: low ($CTP \geq 680$ hPa), mid-level (680 hPa $> CTP \geq 440$ hPa), and high ($CTP < 440$ hPa) cloud. The multi-model means for the 4xCO2 experiment is given in the top 9 panels, and those for the solp4p experiment are given in the lower 9 panels. Stippling indicates grid cells where 3 out of the 4 models agree on the sign of the change. The data are plotted on a 1-degree grid (sampled for each model using a linear interpolation from the models' innate grid).

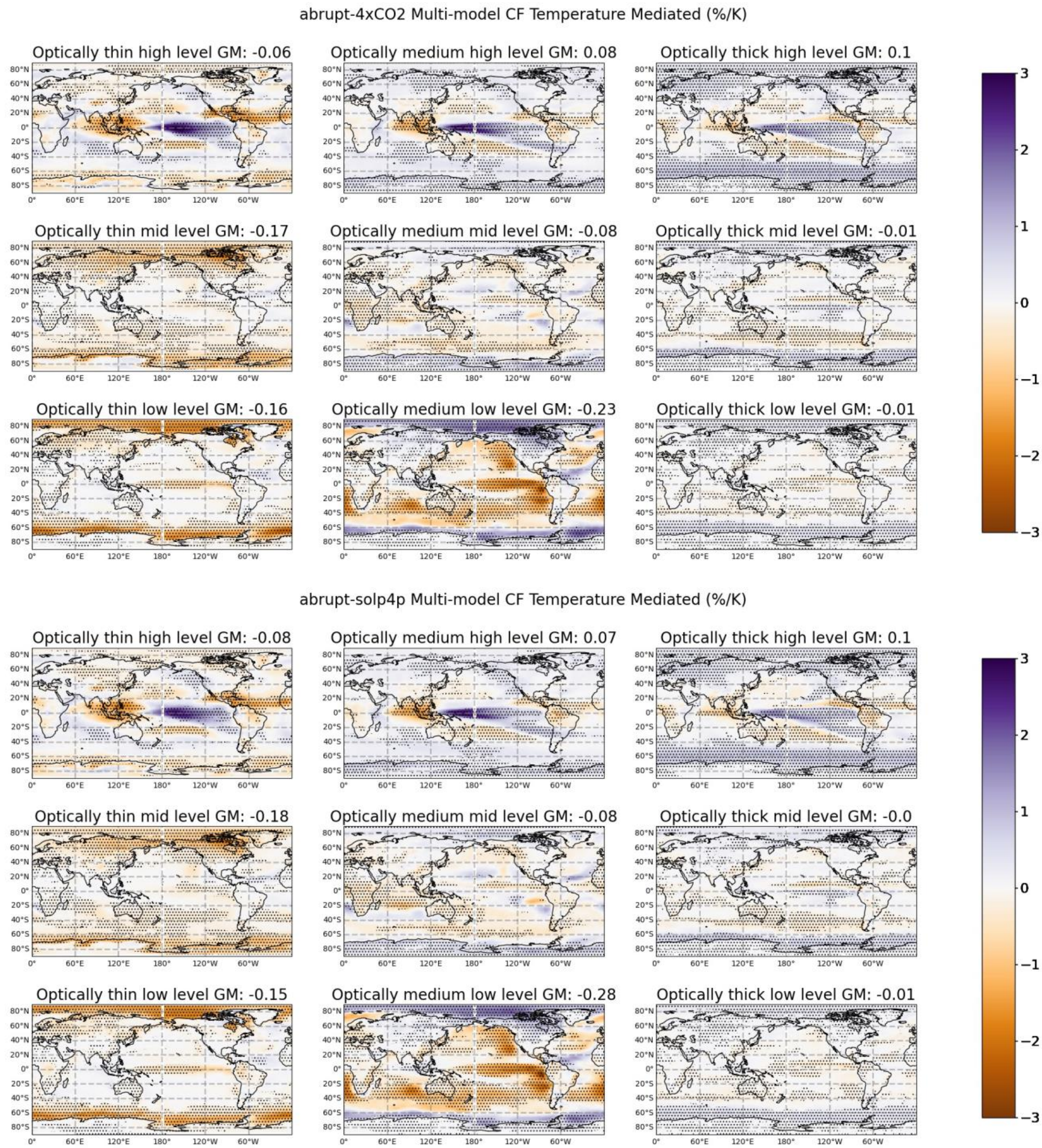

***Figure 2** Temperature mediated response of cloud from the solp4p and 4xCO2 experiments. Colors show the % change in cloud amount in each category per unit of global temperature change, with the global (area weighted) mean change given in the title of each panel. Stippling indicates regions where at least 3 out of 4 models agree on the sign of the temperature mediated cloud change.*

Overall, **Figure 2** shows the pattern of temperature mediated cloud change is quite similar in both the solp4p and 4xCO2 experiments. In fact, while there are significant variations in the pattern between individual models, in each model there is a similar temperature mediated change in both experiments (see **Supplemental Materials** for individual model results). The global mean change is listed in the title of each panel. In the multi-model mean, there is a net reduction in global mean cloud amount in seven out of nine categories with only optically-thick high-level clouds and optically-medium high-level clouds having an increase. Over the next three paragraphs, we discuss the geographic structure of the low, mid, and high-level cloud responses, respectively.

Low clouds: The greatest decrease in cloud fraction with warming occurs in the optically-medium low clouds, where there is large reduction in cloud amount over most oceanic regions equatorward of about 60° latitude. The reduction is especially large in regions that are characterized by relatively cool sea-surface temperatures and large scale subsidence that supports the formation of stratocumulus clouds (Wood, 2012; see **Figures 7 and 9** where stratocumulus regimes are either marked, or can be seen in climatological subsidence rates). In the global mean there is a greater reduction of optically-medium low clouds in the solp4p than the 4xCO2, which is the largest contributor to the greater temperature mediated cloud loss in total cloud amount from solp4p compared with 4xCO2 (as was noted in **Figure 1** and **Table 2**). Poleward of 60° latitude, on the other hand, there is a general increase in the optically-medium low cloud that is accompanied by a decrease in optically-thin low clouds and an increase in optically thick low cloud. This includes the northern half of North America, Siberia, and some interior portions of Eurasia. Reduction of stratocumulus clouds with warming and increases in the optical depth of mid-to-high latitude low cloud has been a well-documented response to increasing CO_2 in both global climate models and process models (Bjordal et al., 2020; Sherwood et al., 2020; Zelinka et al., 2013), and we discuss the associated physical mechanisms in more detail in Section 4.

Mid-level clouds: There are generally smaller changes in the mid-level cloud category than in the low-level and high-level cloud categories. There is nonetheless reduction of midlatitude mid-level clouds that is consistent across models. This reduction is most pronounced in the thin cloud category at mid to high latitudes, however there is a weak reduction in optically medium and thick mid-level clouds that is consistent between models in some regions (including in the Southern Hemisphere midlatitudes), but there is poor model agreement in most regions. There is also a slight increase in optically medium mid-level cloud in the Peruvian and Californian stratocumulus regions of some models, albeit with poor model agreement, which suggests that in some models there is a rising of the stratocumulus layer with increase in global mean temperature. The role of mid-level clouds in climate feedbacks has received less attention than that of high or low-level clouds (Sherwood et al., 2020), and we will return to this in Section 4.

High clouds: In the equatorial Pacific, the temperature mediated response of high clouds in both the solp4p and 4xCO2 experiments form a clear dipole, with increasing high cloudiness over the central and eastern portion of the equatorial pacific and a decrease in high cloud over the western pacific and maritime continent. This pattern is consistent with a weakening Walker circulation. There is also a northeastward shift of the SPCZ, and a reduction of high cloud over the Amazon and central America, which are responses that have been observed to be correlated with the phase of the El Nino Southern Oscillation (ENSO) (Adames & Wallace, 2017). Sea-surface temperature variability of ENSO, and the Atmospheric variability of the Walker circulation are strongly coupled phenomena (e.g. Battisti et al., 2019; Bjerknes, 1969), as such we find these high cloud changes in the Tropical Pacific to be linked with the change in SST pattern with warming (see Section 3.4).

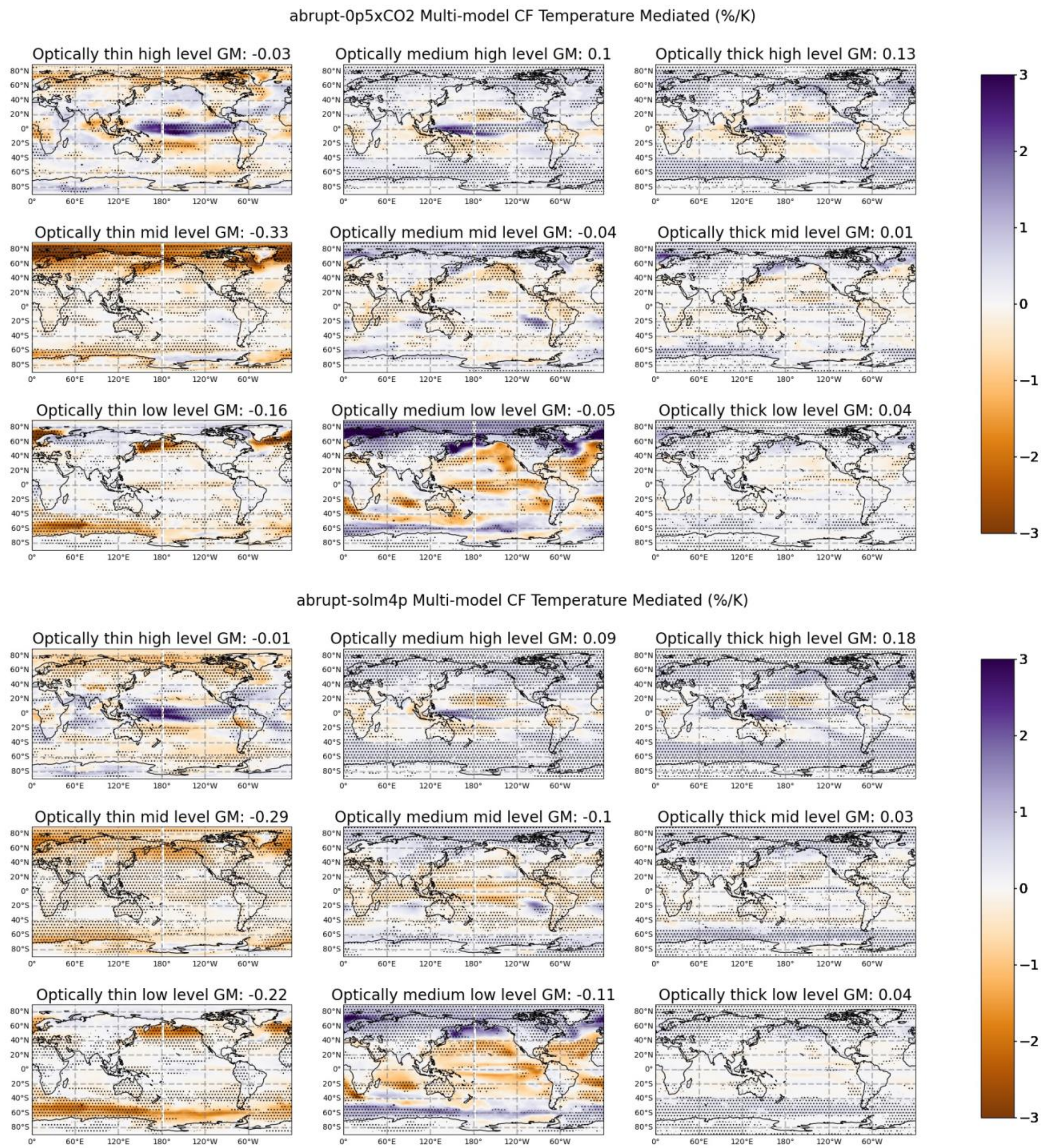

***Figure 3** Temperature mediated response of cloud from the 0p5xCO2 and solm4p experiments shown in the same form as **Figure 2,** except that in the solm4p stippling indicates agreement from at least 2 out of 3 models (as opposed to 3 out of 4 models for the other experiments). Note that these cloud changes are on a per temperature basis, so positive temperature mediated values in these experiments corresponds to cloud loss during the simulations.*

Turning attention to the cooling experiments, **Figure 3** shows the temperature mediated cloud change in the solm4p and 0p5xCO2 experiments. The panels in **Figure 3** follows the same format as **Figure 2,** where the ISCCP simulator histograms have been separated into 9 cloud categories. Note that these cloud changes are on a per temperature basis, so positive temperature mediated values in these cooling experiments correspond to cloud loss as the global temperature decreases. Accordingly, locations with a temperature mediated cloud change that is of the same sign in the warming and cooling experiments means that the actual change in cloud amount is in the opposite direction. For example, such a response occurs in the optically medium low-level clouds over much of the midlatitudes, subtropical, and tropical oceans, where all simulations show a negative temperature mediated response (orange color) indicating that in these areas there is decrease in this low cloud with warming and an increase with cooling. Likewise, the positive temperature mediated response (purple color), such as over Siberia, means an increase in this low cloud with warming and a decrease with cooling. The following two paragraphs discuss differences between the cloud changes in solm4p and 0p5xCO2, and the differences in cloud changes occurring during warming and cooling, respectively.

Solm4p vs 0p5xCO2: While the cooling patterns from solar and CO_2 forcing share some similarity, it is noteworthy that there are larger differences in the low-cloud response between the 0p5xCO2 and solm4p experiments than between the two warming experiments. Specifically, the global mean response for optically medium mid-level and low-level clouds is about half as strong in the 0p5xCO2 experiment (-0.04 and -0.05 %/K respectively) as compared with the solm4p (-0.1 and -0.11 %/K). In the 0p5xCO2 there is a strong increase of low clouds across the Equatorial Pacific with weak changes in the adjacent subtropics, while in the solm4p, there is a weak response in the tropics with poorer model agreement (note less stippling in the solm4p response). There is also an increase in low cloudiness in the Northern Pacific of the solm4p experiment that does not occur to the same extent in the 0p5xCO2 experiment. As previously noted, the solm4p and 0p5xCO2 experiments have different amounts of forcing, and thus different amounts of temperature change. There have been studies on differences in temperature mediated cloud changes from various amounts of CO_2 forcing, such as Bloch-Johnson et al. (2021) who found that models with the greatest nonlinearity in their response to different amounts of forcing, have the greatest differences in the temperature mediated cloud changes with different amounts of warming (i.e. $M(\theta,\phi)$ from Equation 2 is different depending on ΔT). Additionally, sub-polar low clouds contribute to this non-linearity through the saturation of mixed-phase clouds with warming, or in our case with cooling (Bjordal et al., 2020). Thus, we cannot easily separate the differences between the two cooling experiments that arise due to the different forcing mechanism (solar vs CO_2) and the differences in the amount of cooling.

Warming vs. Cooling: While similar in some respects, the pattern of low-cloud response is not quite the same between the warming and cooling experiments. In the warming experiments there is a transition between negative (orange) and positive (purple) temperature mediated cloud response in optically medium and optically thick low-clouds near 60° latitude (in both hemispheres) while in the cooling experiment the transition occurs near 40° latitude; and likewise, the increase in low-clouds over the northern portions of North America and Eurasia is stronger in the cooling experiments. The reduction of optically thin low-level cloud is also about

20° closer to the poles in the warming experiments than the cooling experiments. In fact, in the cooling experiments, the response in optically thin mid-level cloud is the largest of the nine categories, whereas in the warming experiments it is the optically medium low clouds which have the largest change. Turning our attention to the high-level clouds, in the Tropical Pacific there is a very different response in the cooling experiments than occurs in the warming experiments. In the cooling experiments, there is a decrease in high clouds (a positive temperature mediated response) throughout the equatorial pacific, and an increase in high clouds in the subtropics (negative temperature mediated response). This pattern is consistent with a strengthening of the Hadley circulation and the associated intertropical convergence zone (ITCZ) and differs from the warming experiments which show a pattern of change more consistent with a change in the Walker circulation. The circulation changes are further discussed in Section 3.3.

3.2 Top of Atmosphere Cloud Radiative Effect

Thus far we have examined changes in clouds that occur in models forced with abrupt changes of insolation and CO_2 concentration. The cloud changes previously described alter the Earth radiation budget, and thereby feedback on the climate to enhance or diminish the impact of the forcing. The Cloud Radiative Effect (CRE) can be calculated in many ways such as directly from top-of-atmosphere radiation output (Su et al., 2010), Partial Radiative Perturbation (Taylor et al., 2007), or cloud radiative kernels (Zelinka et al., 2012a). Here we use the latter because it provides the most direct link between cloud changes and radiation. Note however that CRE from radiative kernels is calculated directly from changes in the underlying cloud distribution, thus it is independent of cloud masking (see Zelinka et al., 2013). In the solar forcing model simulations, the shortwave kernels are multiplied by 1.04 and 0.96 for the solp4p and solm4p simulations respectively. The effect of this adjustment is small and has no impact on the conclusions. The multi-model mean CRE change due to temperature mediated cloud changes is shown in **Figure 4**. In the next several paragraphs we discuss the tropics, subtropics, and mid-to-high latitudes respectively.

Tropics: In the tropical pacific, the high cloud response shown in **Figure 2** (for both the solp4p and 4xCO2 experiments) creates a dipole structure across the central and western pacific in the SW and LW CRE. Interestingly, that structure cancels in the NET CRE, and what remains is an overall positive radiative effect (meaning less energy is allowed to escape the atmosphere, and there is net positive feedback with increased warming). To further connect the cloud changes to the induced CRE change, we separate the CRE change into three categories: those due to changes in cloud amount, CTP, and cloud optical depth using the kernel decomposition method developed by Zelinka et al. (2012b). The temperature mediated changes in CRE due to changes in CTP, cloud amount, and optical depth are shown in **Figure 5** for the solp4p and solm4p experiments. A similar figure for the 4xCO2 and 0p5xCO2 experiments is available in the **Supplemental Materials**. The decomposition of the CRE into contributions from each component indicate that in the solp4p the total net positive feedback in the central and eastern tropical Pacific is primarily due to the LW effect of rising cloud tops with warming (which dominates over the SW effect of increasing cloud fraction). Perhaps the most well understood effect of climate warming on clouds is that the height of deep convective cloud tops will rise in the atmosphere as the surface warms such that cloud-top-temperature will remain nearly fixed, creating a positive LW cloud feedback (Hartmann & Larson, 2002; Zelinka & Hartmann, 2010). The slowing of the Walker circulation is also likely creating a greater amount of high-cloud formation in the East Pacific, and thus an increase in the average CTP, causing a positive LW feedback. In the western Pacific of the solp4p there is little effect from CTP changes, and CF changes largely cancel in the SW and LW, leaving a small net negative feedback due to increases in optical depth in the multi-model mean. Individual models differ significantly in the strength of the optical depth feedback over the tropical western Pacific. In contrast, in the cooling experiments the effect of changes in CTP is more narrowly confined around the equator than in the warming experiments and has a structure more consistent with a change in the Hadley cycle (more on this in Section 3.3).

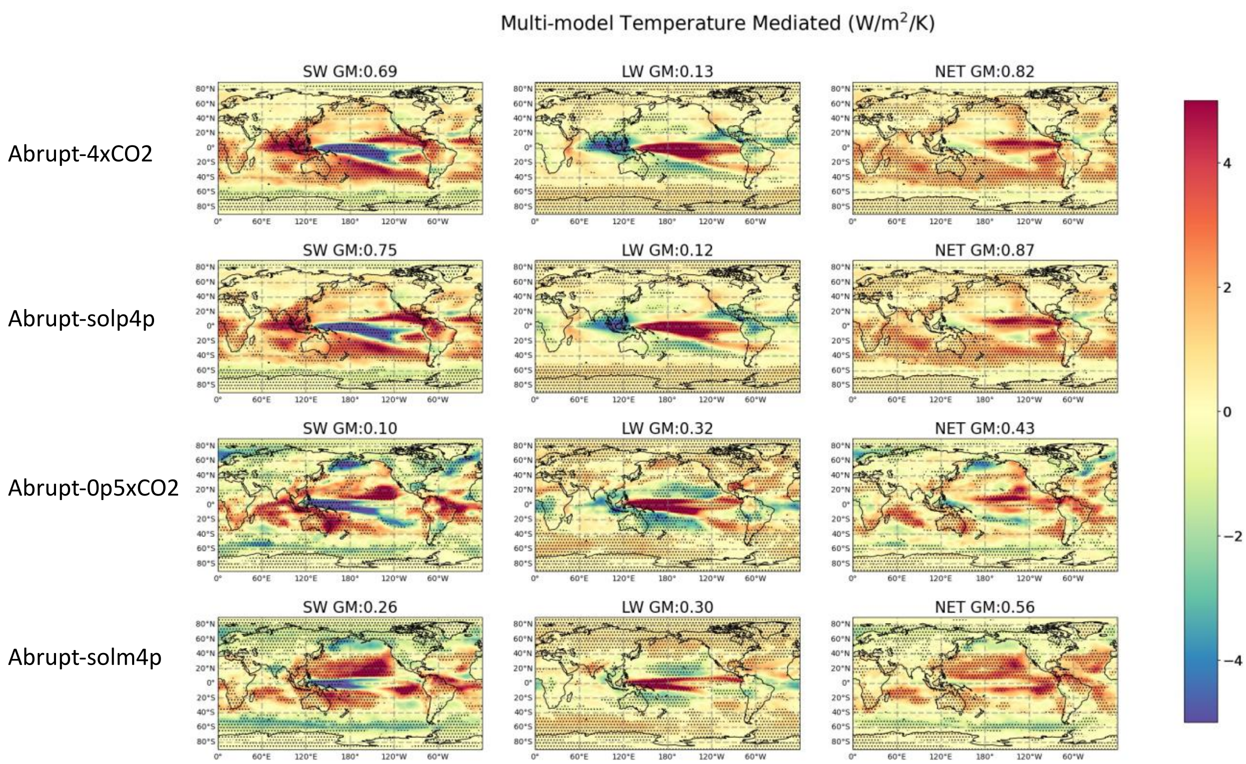

Figure 4 *Multi-model mean temperature mediated cloud radiative effect found using cloud radiative kernels, where downward radiative flux is defined as positive. As with previous figures, stippling indicates model agreement. For the solm4p and 0p5xCO2 experiments a positive temperature mediated feedback corresponds with a decrease in downward radiative flux because of the negative temperature change during those experiments.*

Subtropics: In the subtropical stratocumulus zones (off the west coasts of California, Peru, Namibia, and Australia) in the warming experiments there are strong positive SW radiative feedbacks (**Figure 4**). This is due to changes in cloud fraction (**Figure 5)**, predominantly in the optically medium low-level cloud category (see **Figure 2**). This feedback is present in the cooling experiments, but to a lesser degree. The cooling experiments yield a compensating increase in optically medium mid-level cloud in these regions, such that the temperature mediated change in the combined mid-level and low-level cloud amount is less than in the warming experiments. Outside of the stratocumulus zones, the warming experiments show a large net positive feedback in the Southern Hemisphere between about 20 and 40° S in the Pacific, Indian, and Atlantic basins that is not present (or much weaker) in the Northern Hemisphere and in the cooling experiments. Indeed, the solm4p shows a larger reduction in cloud amount (and positive feedback) in the Northern Hemisphere subtropics than in the Southern Hemisphere subtropics. The strong positive Southern subtropical feedback in the warming experiments is due primarily to a change in the SW CRE, and results from a reduction in optically medium low-level cloud fraction, but also with a noteworthy contribution from an increase in CTP with warming. Zelinka et al. (2020) show that the low-cloud feedback is more strongly positive in CMIP6 around 40° S than at any other latitude, and that this feature is stronger in CMIP6 models than the previous generation, CMIP5.

Mid-to-High Latitudes: In the cooling experiments, there is strong negative SW and a NET negative radiative feedback in the mid-to-high latitudes, poleward of about 40° in both hemispheres, over ocean. This is due to an increase in cloud optical depth (**Figure 5**), and impacts primarily the SW radiation because the change occurs primarily (but not exclusively) in low-level clouds, and appears in **Figure 3** as an increase (orange colors) in the optically thin mid and low-level clouds response to decreasing temperatures, and a corresponding decrease in the optically medium and thick cloud response (purple colors). The same optical depth feedback is present in the warming experiments but occurs poleward of about 60°. More generally, there is a negative SW feedback due to changes in cloud optical depth over land in the cooling experiments, specifically in Northern Canada and Eurasia, as well as in the Arctic and Antarctica, however the NET response to cooling is weaker over land than over ocean because changes of high cloud optical depth create an offsetting LW feedback. To some degree, and again further poleward, the same is true in the warming experiments, but the LW effect associated with thickening of mid and high-level clouds is larger and makes the NET radiative change due to optical depth changes slightly positive. At such high latitudes there is less annually averaged insolation, and there is frequent sea-ice and terrestrial snow cover, such that the SW radiative effect of the cloud optical depth transition is much smaller in the warming experiments.

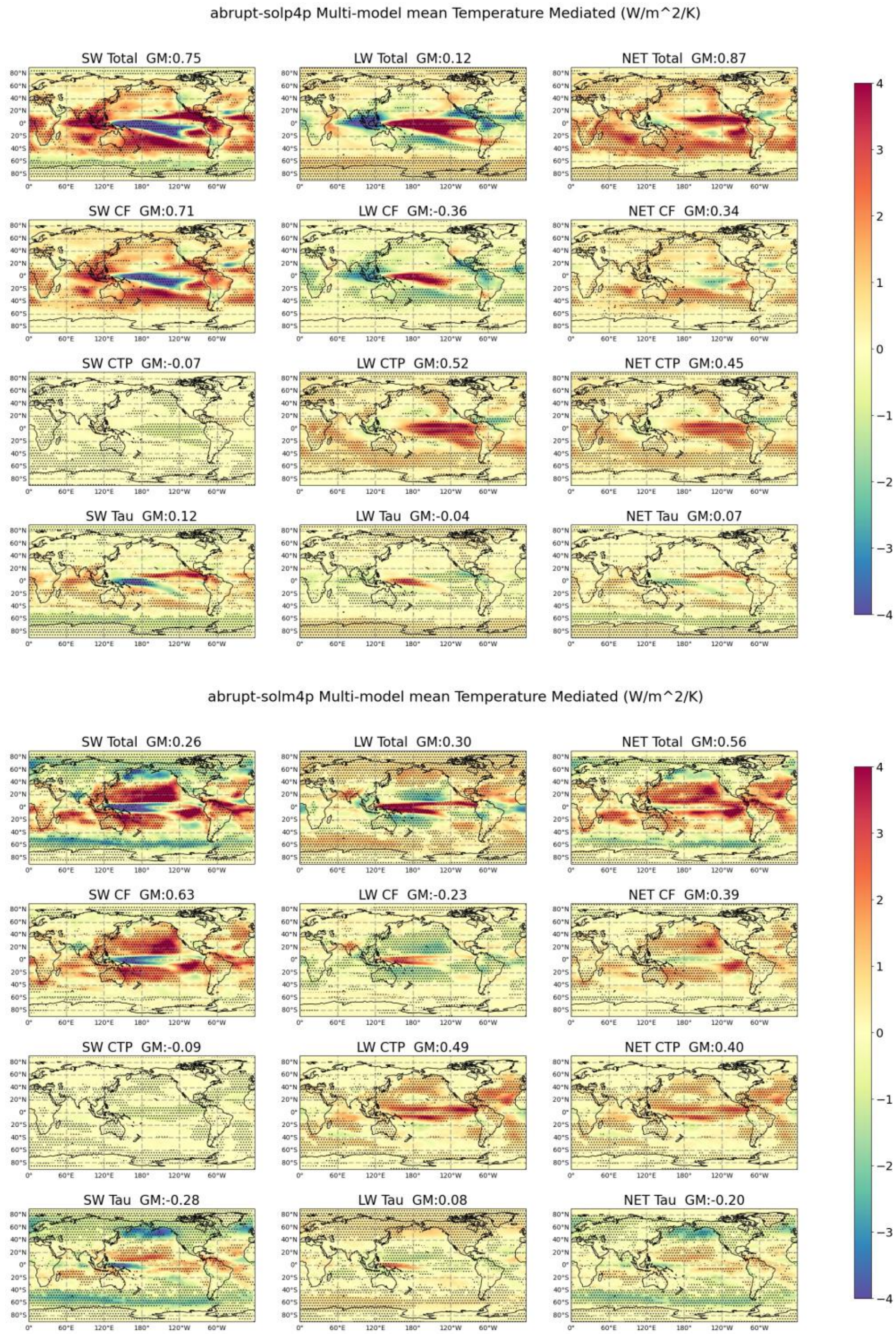

Figure 5 *Multi-model mean cloud radiative effect (CRE) from temperature mediated changes in all cloud changes (Total; rows 1 and 5), cloud top pressure (CTP; rows 2 and 6), Cloud Fraction (CF; rows 3 and 7), and optical depth (tau; rows 4 and 8) in the solp4p (top 4 rows) and solm4p (bottom for rows) model experiments. As in previous figures, stippling indicates regions where there is good agreement among models on the sign of the temperature mediated*

change. The left column is the shortwave component, middle column is longwave, and right column is the net feedback.

The decomposition of the CRE temperature mediated changes for each experiment is shown in the global mean in **Figure 6**, where the bar represents the multi-model mean and the symbols signify the feedback values for individual models.

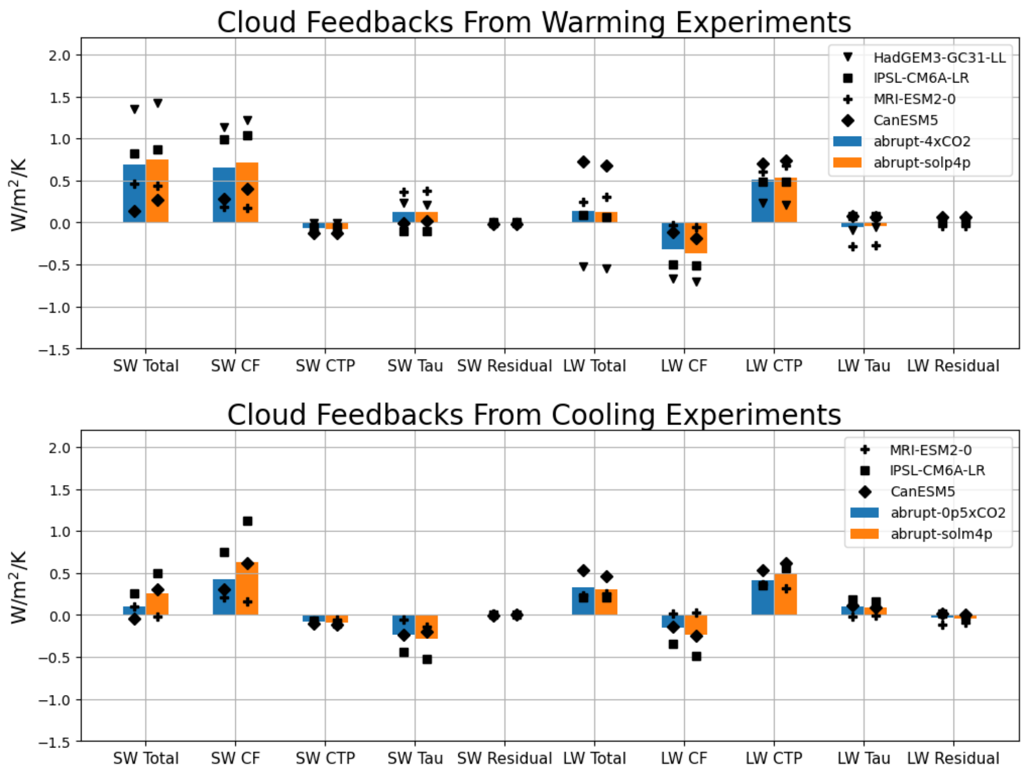

Figure 6 *Global mean temperature mediated cloud radiative feedbacks decomposed into the feedbacks due to three different types of cloud changes (and a residual term). Bars indicate the multi-model mean, black symbols mark the individual models. The top panel shows the solp4p and 4xCO2 experiments while the lower panel shows the solm4p and 0p5xCO2 experiments.*

Figure 6 shows that the LW temperature mediated changes are similar between the 4xCO2 and solp4p experiments in the global mean (which is not surprising given the strong similarity in the clouds responses shown in **Figure 2**). In the warming experiments all models exhibit negative LW feedbacks associated with changes in cloud fraction (which is indicative of cloud fraction reduction allowing more LW flux emitted from the surface to reach space in the global mean), and stronger positive LW feedbacks associated with changes in CTP (which is indicative of clouds forming higher in the atmosphere). In fact, all models performing all 4 experiments produce a positive LW CTP feedback. The LW feedback associated with cloud fraction is consistently more negative across models in the solp4p experiment than the 4xCO2.

The differences are relatively small compared to the intermodal spread of the feedbacks, but they are consistent across all models.

The cloud fraction changes are (by a wide margin) the largest contribution to SW temperature mediated feedbacks in both warming experiments. All models have positive SW cloud fraction feedbacks, which is consistent with the overall reduction of cloud amount that occurs in all models in **Figure 1**. Most models have a small optical depth and CTP components of the SW cloud feedbacks, and all models have positive total SW cloud feedbacks in both warming experiments. Similar to the LW cloud fraction feedback, in the SW there is consistently stronger feedback in the solp4p than the 4xCO2. Although the feedback patterns are quite similar in the two experiments, the total temperature mediated low-cloud reduction is slightly larger in the solp4p experiment this point is discussed further in Section 4.

The lower panel of **Figure 6** shows the cloud feedback decomposition for the solm4p and 0p5xCO2 experiments. There are relatively large differences between the two cooling experiments, as compared to the warming experiments. The 0p5xCO2 experiment produces less feedback associated with change in cloud fraction in the global multi-model mean when compared with either the warming experiments or the solm4p. In the solm4p experiment the SW cloud fraction component is of similar amplitude to the SW cloud fraction component of the 4xCO2 and solp4p experiments. In both cooling experiments there is a relatively strong negative SW feedback from cloud optical depth change (meaning clouds become thinner with cooling in the global mean), which contrasts the warming experiments which have positive SW cloud optical depth feedback (meaning clouds also become thinner with warming in the global mean). Such a difference results in less positive total SW cloud feedbacks in the cooling experiments than the warming experiments.

3.3 Circulation Changes

In this section we examine metrics related to the Hadley and Walker circulations to contextualize the cloud changes described in Section 3.1. In Section 3.1 we found that the temperature mediated changes of high clouds in the tropics are dominated by patterns which are consistent with changes in the Walker and Hadley circulations. In **Figure 7** we show maps of the temperature mediated change in 500 hPa vertical velocity (units are pressure change per day per kelvin), as well as a line plot showing the zonal mean 500 hPa vertical velocity averaged over years 10 to 150 of the simulations. Due to the per-temperature basis of the temperature mediated changes the sign convention of the map plots is such that regions with upward (negative pressure velocity) temperature mediated velocity anomalies (purple color) have more upward motion (more convection or less subsidence) in the mid-troposphere in a warmed climate (solp4p and 4xCO2 experiments) and less upward motion in a cooled climate (solm4p and 4xCO2 experiments). Not surprisingly, the temperature mediated changes in 500 hPa vertical velocity correlates well with the high cloud changes shown in **Figures 2 and 3** in the tropics and subtropics. In all experiments there is negative pressure velocity (increase in upward motion or decreased subsidence) per degree of warming (purple colors) in the central equatorial pacific (at least between 150 E to 150 W) and positive pressure velocities (decrease in upward motion) per degree of warming (green colors) over Indonesia and the Maritime continent, along the northern edge of the ITCZ (and to a lesser degree the adjacent subtropics), and along the southwestern edge of the SPCZ. In at least three models the positive pressure velocity changes over the Maritime region extend well into the Indian Ocean. The cooling experiments differ notably from the warming experiments, and have relatively little change (less purple, less stippling) in the East Pacific and along the Pacific Cold Tongue, as well as over the Peruvian stratocumulus zone.

The positive pressure velocity changes along the northern edge of the ITCZ and southwestern edge of the SPCZ are indicative of the ITCZ and SPCZ shifting equatorward and to the east with warming (and opposite direction with cooling). The shift of the ITCZ and SPCZ is perhaps more easily seen in the zonally averaged 500 hPa vertical velocity (bottom panel of **Figure 7**. The latitude where zonal mean upward motion is maximized (there is a minimum in pressure velocity) in each hemisphere is noted by vertical dashed lines for each model experiment. In the warming experiments there is an equatorward shift of the latitude of maximum updraft (minimum in pressure velocity) in the Pacific in both the northern and southern hemisphere. However, the distance shifted is far greater in the southern hemisphere. There is also a significant increase in convection (a much more negative pressure velocity) in the southern hemisphere tropics and an associated increase in subsidence in the southern subtropics (20° to 40° S) relative to the control simulation, whereas in the northern hemisphere there is a decrease in tropical convection and a decrease in subsidence in the adjacent subtropics.

In the solm4p and 0p5xCO2 experiments the opposite shift in convection does occur compared to the warming experiments, however it is not of equal magnitude. In the southern hemisphere the latitude of maximum convection (minimum in pressure velocity) shifts poleward with cooling by the same amount in the solm4p and 0p5xCO2, however the shift is of much shorter distance than the equatorward shift in the two warming experiments. Additionally, there is little change in the amount of convection and subsidence in the tropics and subtropics of the southern hemisphere due to cooling. In the northern hemisphere the tropical convection shifts poleward in the solm4p, but there is no change in the location of maximum convection in the 0p5xCO2 experiment. Both cooling experiments produce an increase in the strength of the northern hemisphere tropical convection, and an increase in subsidence in the adjacent subtropics.

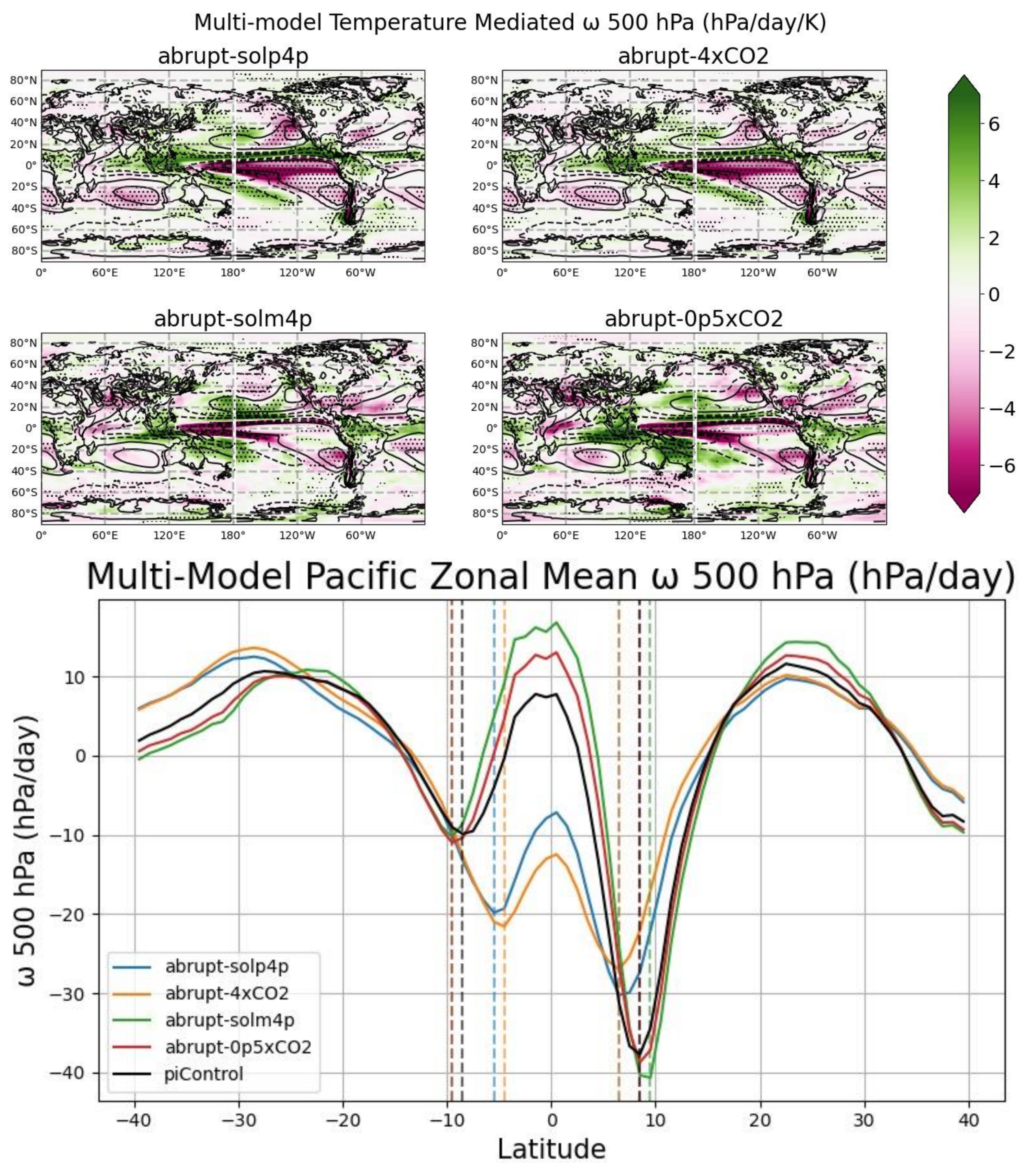

Figure 7 *Top 2 rows: multi-model means of 500 hPa vertical velocity. Contours are the pre-industrial climatology with contour intervals of 20 hPa/day. The coloration of these maps are the temperature mediated change in 500 hPa vertical velocity. Bottom: Pacific zonal mean climatologies of 500 hPa vertical velocity, averaged over ocean area from 120° W to -60° E . Vertical dashed lines indicate the latitude of maximum mean upward velocity in each hemisphere. Note that in the Northern Hemisphere this occurs at the same latitude for the piControl and 0p5xCO2, and in the Southern Hemisphere this occurs at the same latitude for the solm4p and 0p5xCO2.*

Much of the upward motion in the tropics is related to the large-scale dynamical circulations that occur in both the zonal and meridional directions. **Figure 8** shows the zonal mean 500 hPa meridional stream function, which has been widely used to diagnose the strength and width of the zonally overturning Hadley circulation (e.g. Chemke, 2022; Frierson et al., 2007; Oort & Yienger, 1996; Staten & Reichler, 2014). We have separated the stream function into the DJF and JJA seasons because the Hadley circulation, in fact, only occurs in the Winter Hemisphere, so annual mean plots can misleadingly depict the Northern and Southern node of the Hadley circulation simultaneously. The strength of the Hadley circulation is often quantified as the maximum absolute value meridional stream function at 500 hPa (e.g. Oort & Yienger, 1996). **Figure 8** shows that the Hadley circulation weakens in both the solp4p and 4xCO2 and strengthens in the solm4p in both DJF and JJA. In the 0p5xCO2 experiment there is a small increase in the Hadley circulation strength in DJF, however there is little change in JJA. As such, the high cloud changes in the Southern Hemisphere of the 0p5xCO2 experiment are apparently unrelated to changes in the strength of the Hadley circulation.

The Hadley circulation width can be characterized using the latitude where the 500 hPa stream function crosses the zero line. By this metric, the Hadley cell widens in the warming experiments and shrinks equatorward in the cooling experiments. Because the width changes can be small and difficult to see in **Figure 8**, the Hadley cell width in each season (and associated hemisphere) calculated from the last 30 years of each simulation is shown in **Tables 4 and 5**. In all models there is a widening of the Hadley circulation in both hemispheres and in both the 4xCO2 and solp4p. Neither of the warming simulations has a Hadley circulation that is persistently wider than the other across all models.

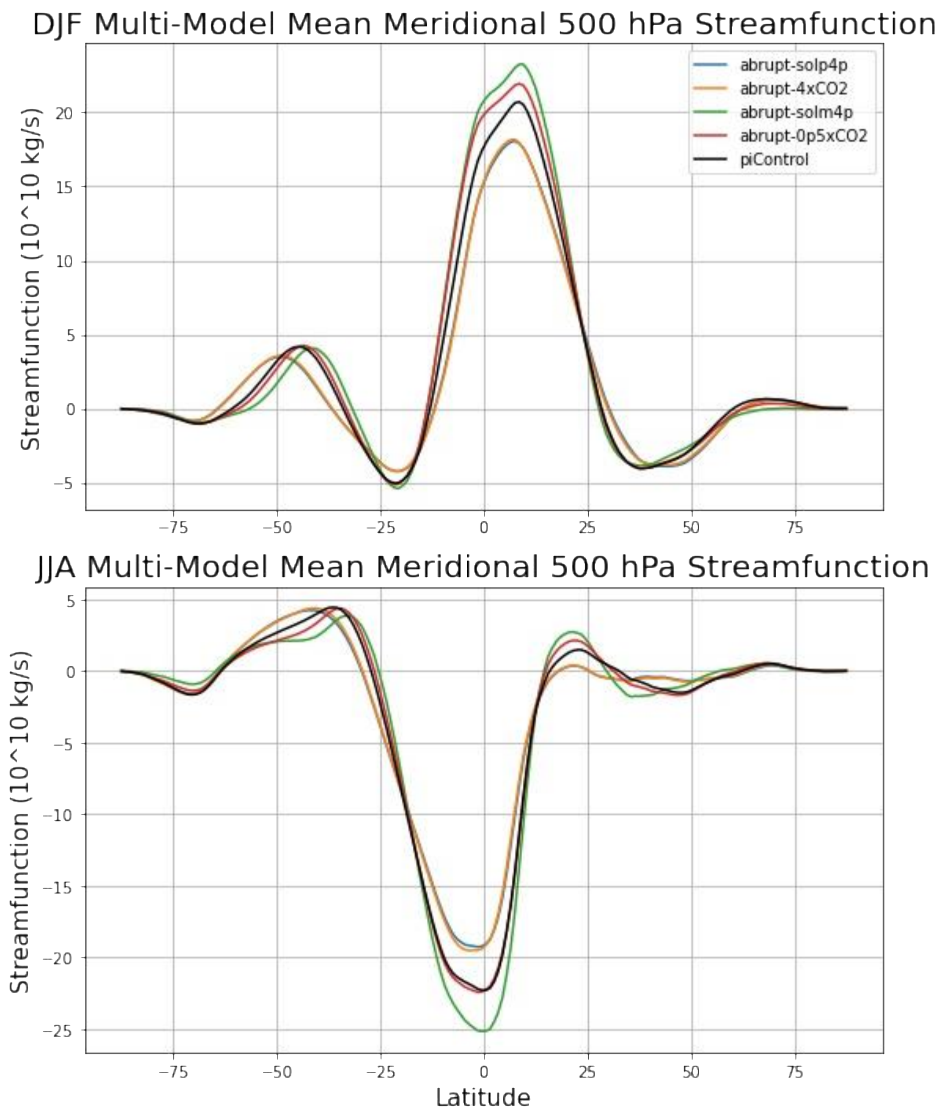

Figure 8 *Zonal mean 500 hPa meridional streamfunction shown as averages over the final 30 years of each model experiment.*

In the 0p5xCO2 and solm4p experiments there is some cooling in the East Pacific relative to the West Pacific, however the change in the temperature gradient across the equatorial Pacific is weaker than in the 4xCO2 and solp4p experiments. In southern subtropical Pacific there is generally a smaller temperature change than in the global mean. The relatively warm subtropical surface air temperatures are collocated with an increase in high cloud amount and contributes to the South-Western shift of the SPCZ. Narsey et al. (2022) found that in CMIP5 and CMIP6 models the SPCZ shifts towards the region with relatively high surface temperatures under warming due to the associated shift of the midlatitude jet. Thus, we expect that when cooling occurs the same mechanisms apply, and the SPCZ shifts towards regions with relatively less cooling. In the following subsection, we continue to investigate the physical mechanisms that contribute to cloud feedbacks in the solar and CO_2 forced experiments by examining surface temperature patterns.

Hadley Cell Width (° Latitude)					
Experiment	**piControl**	**Abrupt-4xCO2**	**Abrupt-solp4p**	**Abrupt-0p5xCO2**	**Abrupt-solm4p**
MRI-ESM2-0	28.1	28.8	29.1	27.8	27.3
IPSL-CM6A-LR	28	30	29.2	28.1	27.8
CanESM5	29.5	31.8	32.7	29.2	29
HadGEM3-GC31-LL	28.3	30.4	30.8	27.8	NA
CESM2	28.7	30.9	30	28.7	27.7
MM mean	28.5	30.4	30.4	28.3	28.0

Table 4 *Hadley circulation width metric in the Northern Hemisphere during DJF, quantified as the latitude where the 500 hPa meridional stream function crosses zero for the first time in the associated hemisphere. These values are calculated by linearly interpolating the models' latitude grid to the point at which 500 hPa stream function of zero is crossed.*

Hadley Cell Width (° Latitude)					
Experiment	**piControl**	**Abrupt-4xCO2**	**Abrupt-solp4p**	**Abrupt-0p5xCO2**	**Abrupt-solm4p**
MRI-ESM2-0	27.3	28.7	28.7	26.8	26.5
IPSL-CM6A-LR	25.8	28.7	28.3	25.3	24.9
CanESM5	28.2	30.2	31.3	27.6	25.9
HadGEM3-GC31-LL	27.7	30.5	30.7	26.9	NA
CESM2	28.6	32.4	30.4	28	27.3
MM mean	27.5	30.1	29.9	26.9	26.2

Table 5 *Same as Table 4, but for the Southern Hemisphere and JJA season.*

3.4 Surface Temperature

The left side of **Figure 9** contains plots of the temperature mediated change in surface temperature. The zonal temperature gradient across the equatorial Pacific is a strong predictor of the strength of the Walker circulation, because a strong temperature gradient supports easterlies due to the associated pressure gradient. This circulation is fundamentally coupled to the ocean circulation, where the wind stress forces a thermocline gradient, which further supports a sea-surface temperature gradient through upwelling in the East Pacific (Battisti et al., 2019; Bjerknes, 1969). Therefore, we expect that changes in the surface temperature pattern may help explain the zonal structure of the high cloud changes shown in **Figures 2 and 3**. Additionally, Qu et al., (2014) found that sea-surface temperature and Estimated Inversion Strength (hereafter EIS) are two cloud-controlling-factors which are both a strong predictor of low-cloud fraction on monthly-to-interannual timescales, so the surface temperature changes also yield important insight into the causes of low cloud changes.

In the equatorial pacific of the 4xCO2 and solp4p experiments there is enhanced warming (greater warming than the global mean) in the East, and less warming in the West Pacific. In the 0p5xCO2 and solm4p experiments there is some cooling in the East Pacific relative to the West Pacific, however the change in the temperature gradient across the equatorial Pacific is weaker than in the 4xCO2 and solp4p experiments (and has poor model agreement in the cooling experiments). This difference in sea-surface temperature patterns likely explain much of the differences in the high cloud response to warming and cooling seen in **Figures 3 and 4**.

On land there is generally greater warming than in the adjacent oceans in the 4xCO2 and solp4p experiments. Enhanced warming over land is a well-documented response in models and is constrained by the differences in lapse rate over land and ocean, owing to the greater moisture availability over ocean. Further details on such mechanisms are described by Byrne & O'Gorman (2013) and Joshi et al. (2008). Interestingly, in the 0p5xCO2 and solm4p there is little difference between the ocean and land cooling, especially in the Southern Hemisphere. This suggests that the oceanic and continental lapse rate adjustments to cooling exhibit lesser differences than their adjustments to warming.

Over the subtropics, there is smaller surface temperature change than the global mean (blue colors) in all four model experiments. In the warming experiments there is less warming in the Northern Hemisphere subtropics relative to the Southern Hemisphere subtropics, and the opposite in the cooling experiments. We note that local surface temperature is an important cloud controlling factor in the midlatitudes and subtropics.

We find that over the ocean in the Southern Midlatitudes and much of the Southern Subtropics there is greater warming than the global mean in the 4xCO2 and solp4p, as well. This region has been the subject of research by Zelinka et al. (2020) who show that such enhanced warming is associated with low cloud reduction.

3.5 Estimated Inversion Strength

To better understand low cloud changes, we show in the right panels of **Figure 9** maps of temperature mediated changes in estimated inversion strength (hereafter EIS). Stratocumulus cloud occurrence in particular is typically very well correlated with EIS on monthly or longer time-scales, especially in the Tropics and Subtropics (Wood & Bretherton, 2006). In the right panels of **Figure 9** we have highlighted a few subtropical regions with red boxes where there are persistent stratocumulus cloud in the modeled piControl climatology, and observations (Klein & Hartmann, 1993; Qu et al., 2014, 2015). But stratocumulus are also common over colder waters at mid and high latitudes, especially in the winter (Wood, 2012).

In the warming experiments there is increasing EIS in the northern hemisphere tropics and parts of the subtropics. Especially from 0° to 20° in the Central and Eastern Pacific, and Atlantic oceans. Additionally, there is an increase of EIS in the Eastern Atlantic, off the west coast of Northern Africa and Europe. In the southern hemisphere increases in EIS are less widespread. There is narrow region of EIS increase primarily along a line connecting Indonesia to the Peruvian stratocumulus deck (denoted as the red box off the west coast of South America). In the midlatitudes of both hemispheres (poleward of 40°) and along the equator in the Eastern and Central Pacific, there is also notable decrease of EIS. In the stratocumulus regimes (marked with red boxes) there are inconsistent changes in EIS, where some stratocumulus regimes experience strengthening inversions, while others experience weakening with increasing temperature. For example, there is decreasing EIS over most of the Californian, Peruvian, and Australian stratocumulus regions, and increasing EIS in the African and North Atlantic Stratocumulus. We note that in all these regions there is a decrease in low cloud amount (see **Figure 2**), the role of EIS in contributing to such changes are further discussed in **Section 4**. The temperature mediated EIS changes shown here broadly agree with the late stage temperature mediated changes of EIS in CMIP5 model simulations of 4xCO2 found by Qu et al. (2015), and the differences that occur are attributable to the different set of models used in each study.

In the cooling experiments there are broadly similar patterns of temperature mediated EIS change to the warming experiments, however there are some key differences. In the tropical Atlantic in contrast to the response to warming, there is little EIS change in the solm4p and 0p5xCO2. In the Southern hemisphere there is decrease of EIS in the subtropical Pacific, Atlantic and Indian Oceans with decreasing temperature (green color), which is more widespread than the EIS changes in the southern hemisphere caused by warming. Like the warming experiments, in the stratocumulus regimes the EIS is not consistently increasing or decreasing. There is decreasing EIS with cooling (green color) in most of the Peruvian and Australian stratocumulus regions and increasing EIS with cooling (pink color) in most of the North American, North Atlantic, and African stratocumulus regions.

3.6 Relative Humidity

Recent research has shown that in climate models, trade cumulus occurrence is mediated by the moisture fluxes into and out of the boundary layer. As such, drying of the free-troposphere can increase the rate of boundary-layer drying through convective mixing, which desiccates the cloud layer (Vogel et al., 2022). In the right column of **Figure 9** we show the temperature mediated changes in relative humidity at 700 hPa (RH_{700}), which indicates the dryness of the lower portion of the free troposphere.

In the tropics and subtropics of all four experiments there is a strong correspondence between the 700 hPa relative humidity and 500 hPa vertical velocity, such that RH_{700} increases in regions where there are negative anomalies in the mean 500 hPa vertical velocity (upward motion) – and as described in Section 3.3 an increase in high cloud in these regions – and decreases where there are positive anomalies in the mean 500 hPa vertical velocity. And just as the pattern of 500 hPa vertical velocity changes are not the same in warming as cooling experiments, the pattern of RH_{700} differs as well. In the warming experiments there is increased RH_{700} in the Tropical East Pacific and decreased in the Tropical West Pacific, while in the cooling experiments there is an increase in relative humidity (negative temperature mediated change) around 20° north and south of the equator, and a decrease in relative humidity along the equatorial Pacific, Atlantic, and Indian oceans. In the subtropical stratocumulus regions, there is an increase in RH_{700} with warming (green colors), and a more mixed response to cooling. For example, in the solm4p there is increased RH_{700} in the Californian, Peruvian and Australian stratocumulus (purple colors), and in the 0p5xCO2 experiment there are relatively weak decreases with poor model agreement. In the midlatitudes of the warming experiments, there is relatively little change in the Northern Hemisphere between 40° and 60° N and a general drying pattern (purple colors) in the Southern Hemisphere between 40° and 60° S. In the cooling experiments there is also drying (green colors) in various regions of the Southern Ocean.

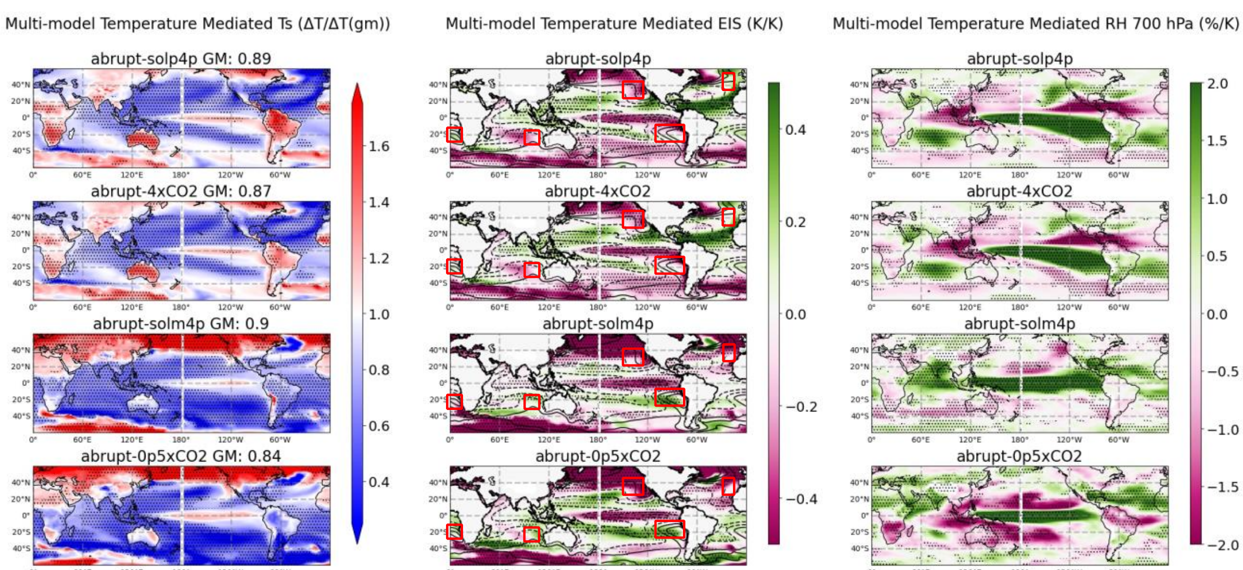

__Figure 9__ Left Panels: Temperature mediated change in surface temperature. Stippling indicates good model agreement on whether the change is above or below 1 K/K(global). Middle Panels: Temperature mediated changes in Estimated Inversion Strength (EIS), contours are the pre-industrial average EIS, red boxes denote known stratocumulus regimes. Right Panels: Temperature mediated changes in relative humidity at 700 hPa. As with previous figures

stippling indicates regions with good model agreement on the sign of the change of both EIS and RH 700 hPa.

3.7 Cloud Phase Feedbacks and Sea Ice-Cloud Interaction

On the left-hand side of **Figure 10** we show the changes in whole-column cloud ice mass fraction, which is the vertically integrated atmospheric ice-mass content divided by the combined mass of ice and liquid water. There is an increase in cloud ice mass fraction in the solm4p and 0p5xCO2 that extends through the midlatitudes down to 30° in the solm4p and to 40° in the 0p5xCO2. In the solp4p and 4xCO2 there is a reduction in cloud ice mass fraction poleward of 50° latitude. The change in cloud ice fraction in each of the four experiments is well collocated with the change in low-cloud optical depth shown in **Figures 2 and 3**.

The right panels in **Figure 10** show the change in sea-ice extent as a thirty-year average deviation from the pre-industrial climatology. In the cooling experiments the sea-ice reaches much lower latitudes than in the pre-industrial climate, where there is sea-ice growth past 50° in both hemispheres of the solm4p and growth past 55° in the 0p5xCO2. In the warming experiments there is a large reduction of sea-ice that reaches Antarctica and the North Pole such that the arctic is nearly ice-free. The effects of both the cloud phase and sea-ice on cloud attributes and radiative effect are discussed in the following section.

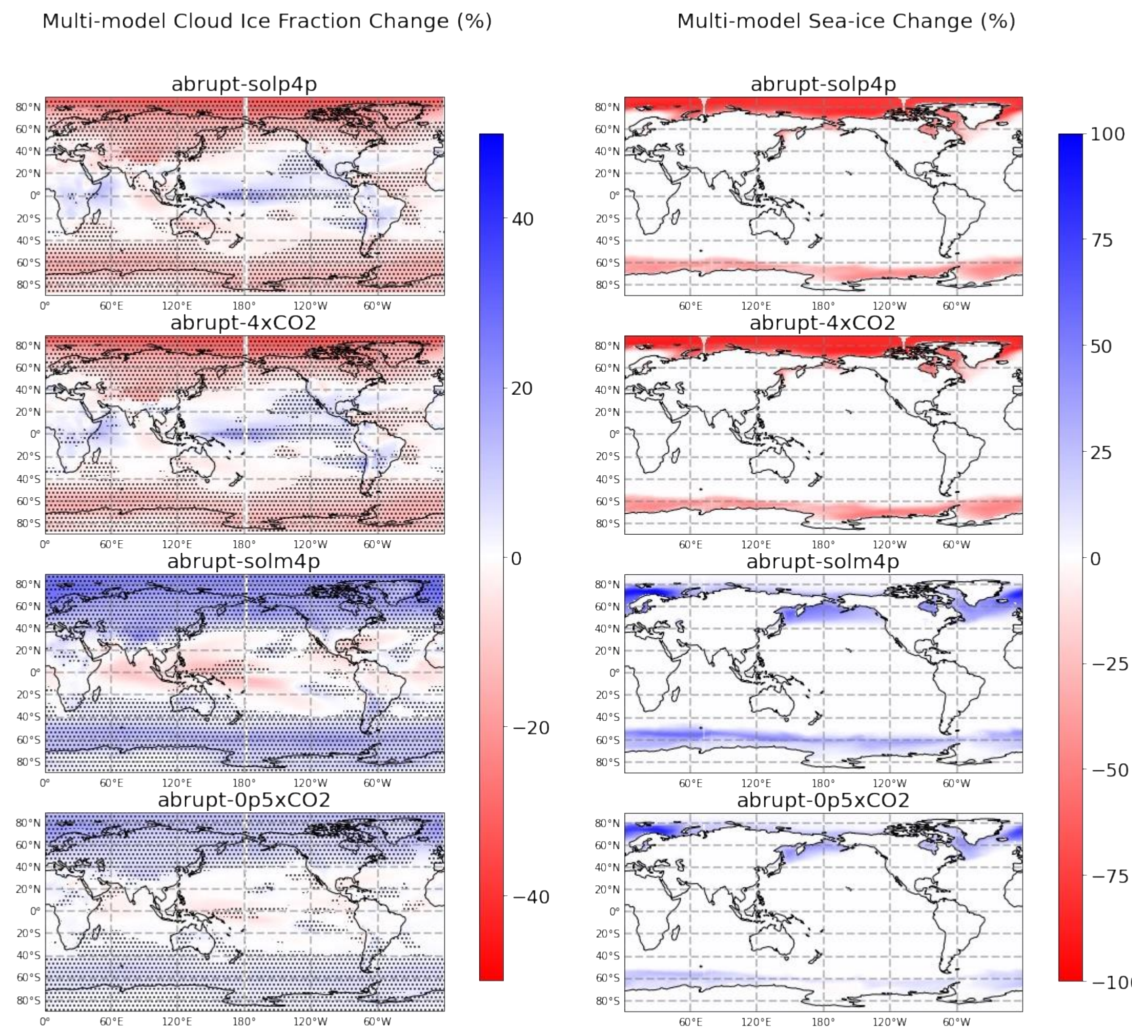

***Figure 10** Left: Multi-model mean change in cloud ice mass fraction shown as the average of the final 30 years of simulation subtracting the pre-industrial average. As in previous figures, stippling indicates regions where there is model agreement on the sign of the change. Right: Multi-model mean change in sea-ice fraction shown as the average of the final 30 years of simulation subtracting the pre-industrial average.*

4 Discussion of Physical Mechanisms

In this section we discuss further the simulated cloud changes and likely mechanisms in the context of previous studies. In turn, we focus on high clouds, low and mid-level clouds, and lastly high latitude clouds. We also briefly discuss some limitations of the radiative kernel approach at the end of this section.

4.1 High Clouds

In the solp4p and 4xCO2 experiments, there is a high cloud change that is indicative of a weakening walker circulation, as well as a shift of the ITCZ towards the equator and a

Northeastward shift of the SPCZ. The cloud changes occur in the same locations as changes in the vertical velocity, indicating that the tropical high cloud changes are in fact circulation driven. A similar circulation pattern occurs during the El Nino phase of ENSO (Adames & Wallace, 2017). In the warming experiments, the increase in tropical surface temperature is largest in the Tropical Central Pacific (see **Figure 9**), similar to the pattern associated with El Nino. Hence, the models trend towards a tropical mean-state that is similar to the El Nino phase of the current climate.

There are a handful of mechanisms which have been proposed to mediate the zonal temperature gradient and associated Walker circulation (Held & Soden, 2006; Knutson & Manabe, 1995; Williams et al., 2023). Each of which predict walker circulation changes consistent with those seen in the warming and cooling experiments analyzed here. Knutson & Manabe (1995) proposed a pair of contributing mechanisms, the first of which is that higher static stability occurs in the warming experiments, which slows the convection in the West Pacific and decreases subsidence in the East Pacific, causing less wind stress along the equatorial pacific, bringing less cool water from the Eastern Pacific into the Central Pacific, and creating a weaker surface temperature gradient between the Central and Western Pacific. We do find higher static stability in the West Pacific (more below on this) and decreased subsidence in the East Pacific (see **Figure 7**) in the warming experiments.

The opposite does not occur (at least not to the same extent) following the abrupt reduction of the solar constant or CO_2, where there is not a clear shift towards a La Nina-like mean state in the solm4p or 0p5xCO2 experiments. In the solm4p experiments the static stability decreases in the West Pacific, but the change is weaker than the increase in the solp4p and 4xCO2 experiments. The multi-model mean static stability anomaly averaged over the final 30 years of simulation in the Tropical West Pacific from 600 to 200 hPa is 0.020 and 0.022 K/hPa in the 4xCO2 and solp4p experiments respectively, and the stability anomaly over the same region is -0.014 K/hPa in the solm4p experiment. The static stability anomaly over this region has a smaller amplitude in the solm4p than the 2 warming experiments in all models (shown in **Table 6**).

This can be understood as a consequence of the moist adiabatic lapse rate, which effectively sets the lapse rate in convective regimes near quasi-equilibrium. The moist adiabatic lapse rate has a nonlinear relationship with surface temperature (due in part to the dependence of the saturation vapor pressure on temperature, and the Clausius-Clapeyron relationship), such that the lapse rate increases more rapidly with increasing temperature. This creates the asymmetric static stability changes in the warming and cooling experiments, and following Knutson & Manabe (1995) causes a greater slowing of the Walker circulation in the warming experiments than there is hastening of the Walker circulation in the cooling experiments.

Static Stability Anomaly (K/hPa)

Experiment	**Abrupt-4xCO2**	**Abrupt-solp4p**	**Abrupt-0p5xCO2**	**Abrupt-solm4p**
IPSL-CM6A-LR	0.023	0.024	-0.008	-0.016
MRI-ESM2-0	0.014	0.015	-0.007	-0.012
CanESM5	0.024	0.032	-0.007	-0.017
CESM2	0.018	0.014	-0.005	-0.01
HadGEM3-GC31-LL	0.019	0.023	0.02	NA
MM mean	0.020	0.022	-0.0014	-0.014

Table 6 *Static Stability averaged over the final 30 years of each simulation in the Tropical West Pacific (120-140° Longitude, -15-15° Latitude) from 600 to 200 hPa.*

The other contribution to Walker circulation changes identified by Knutson & Manabe (1995) is the role of the longwave cooling profile, due to changes in specific humidity of the upper troposphere. In a warmer climate the upper tropospheric cooling rate over the West Pacific increases more than is balanced by convective heating. The net radiative cooling over the West Pacific weakens the pressure gradient aloft that circulates air from the convective West to subsiding East Pacific, weakening the Walker circulation. Only 2 of the models we have examined here saved output of vertically resolved radiative flux, however both models with radiative flux outputs do show a larger increase in LW cooling from the 4xCO2 and solp4p than the reduction in LW cooling in the solm4p experiment (see **Supplemental Materials**). This suggests that the asymmetrical response in the tropical pacific to warming and cooling is consistent with both mechanisms presented by Knutson & Manabe (1995).

In the framework of Held & Soden (2006), a change in convective moisture flux is viewed through the lens of the hydrological budget. Moisture flux (M) is equal to the product of boundary layer specific humidity (q_{BL}; in our case averaged from the surface to 850 hPa), and precipitation (P) such that a change in convective moisture flux is the difference between a change in boundary layer specific humidity, and precipitation.

$$\frac{1}{M}\frac{dM}{dT} = \frac{1}{P}\frac{dP}{dT} - \frac{1}{q_{BL}}\frac{dq_{BL}}{dT} \tag{3}$$

Over the Tropical West Pacific (120-140° longitude, -15-15° latitude), the difference in specific humidity and precipitation changes predicts a multi-model mean temperature mediated change in the convective moisture flux of -6.0 %/K for solp4p, -6.9 %/K for 4xCO2, -1.6 %/K for solm4p, and -3.6 %/K for 0p5xCO2. This is again consistent with a stronger dampening of the Walker circulation and reduced high cloud in the Tropical West Pacific in the warming experiments. We note that the difference in mass flux change calculated using the Held & Soden (2006) framework is mostly due to the boundary layer specific humidity term of Equation 2. In the Tropical West Pacific, the temperature mediated boundary layer specific humidity changes are an increase of 5.9 %/K for solp4p, and 5.6 %/K for 4xCO2, and decrease of 3.4 %/K for solm4p, and 3.6 %/K.

Our findings of a different response in the Walker circulation to warming and cooling is also consistent with the results of Williams et al. (2023), who performed model experiments with warming and cooling patches in the Tropical West Pacific. They use the tropical moist static energy budget to find that nonlinear response to tropical warming and cooling is a direct result of quasi-equilibrium in the ascending portion of the tropical atmosphere, and relatively weak temperature gradients in the tropical free troposphere. They find that cooling reduces the amount of deep convection in the West Pacific, which causes weaker coupling between the Western Pacific boundary layer, and free tropospheric temperature. Such decoupling means that cooling the west Pacific has less impact on the east Pacific than warming, hence there is a weaker Walker circulation change from cooling than warming.

In addition to the zonal (Walker) circulation in the equatorial Pacific, there are also changes in the meridional (Hadley) circulation in the tropics and subtropics. In the solp4p and 4xCO2 there is a weakening and widening of the Hadley circulation (shown in **Figure 8**), that is similar across the two warming experiments. In the solm4p there is a characteristically similar effect in the opposite direction, where in both the Northern and Southern Hadley Cells the circulation strengthens, and narrows. Interestingly, however, in the 0p5xCO2 there is only a change in the Hadley cell strength in the Northern Hemisphere. In the Southern Hemisphere, the Hadley circulation strength and width remains nearly the same as during the pre-industrial climate simulations. This suggests that greater forcing may be necessary to change the Southern Hemisphere Hadley circulation than the Northern Hemisphere circulation. In the 0p5xCO2 there is a narrowing of the Hadley circulation, indicating that even though the strength does not change, the static stability decrease in the subtropics still moves the threshold of baroclinic instability closer to the equator, which drives the Hadley cell boundary (Lu et al., 2007).

There is also a high cloud shift associated with changing locations and strength of the ITCZ and SPCZ. In the subtropical Southern Pacific, the temperature change is smaller than the global mean change. The relatively warm subtropical surface temperatures are collocated with an increase in high cloud amount and contributes to the South-Western shift of the SPCZ. Narsey et al. (2022) found that in CMIP5 and CMIP6 models, the SPCZ shifts towards the region with relatively high surface temperatures under warming. In our case the SPCZ shifts towards the regions with greater warming in the solp4p and 4xCO2, and towards regions less cooling in the solm4p and 0p5xCO2.

There is positive feedback in the tropics of all experiments associated with the change in CTP with warming and cooling, consistent with the Fixed Anvil Temperature (FAT) hypothesis

(Hartmann & Larson, 2002; Zelinka & Hartmann, 2010). Under FAT, the maximum height of deep convection is set by the height at which longwave cooling of the clear-sky atmosphere is no longer efficient. The longwave cooling of the upper atmosphere is predominately due to water vapor, and the spectral properties of the water vapor molecule cause strong radiative cooling to space throughout the troposphere with temperatures above 220 K, and little cooling to space at temperatures below 220 K (Jeevanjee & Fueglistaler, 2020). Thus, when the climate warms deep convective clouds rise in altitude (and vice-versa for cooling climates) keeping convective cloud tops near 220 K. This creates a positive LW cloud feedback because the relative cooling of the cloud top emission temperature remains nearly constant as the surface temperature increases (Hartmann & Larson, 2002; Zelinka & Hartmann, 2010). There is observational support for this feedback, including a recent study we have published on rising cloud tops of high clouds based on stereo-imaging observations from the NASA Multiangle Imaging Spectro-Radiometer (MISR) (Aerenson et al., 2022; Norris et al., 2016). We also find in Section 3.2 that the feedback associated with decreasing CTP is slightly stronger in solp4p than 4xCO2. The difference is small but is consistent with solp4p causing more concentrated warming in the tropics, where deep convection is more common.

4.2 Low and Mid-level Clouds

All of the abrupt forcing experiments produce significant temperature mediated changes in low and midlevel clouds. In the solp4p and 4xCO2 there is a reduction of optically medium low cloud between 40° S and 40° N, especially along the Eastern Pacific cold tongue, and in regions with persistent stratocumulus decks (denoted in **Figure 9**). Stratocumulus clouds form when there is supply of moisture at the surface, the boundary layer is well mixed and has sufficient instability to lift surface air to the condensation level, and the free troposphere is stable enough to cap the instability at a relatively low altitude. Bretherton (2015) identified four feedback mechanisms that cause stratocumulus clouds to change with increased CO_2: 1) *the radiative effect* where an increase in water vapor or CO2 in the free troposphere inhibits cloud top cooling (which stabilizes the boundary layer causing stratocumulus to lower and thin with an increasingly emissive free troposphere), 2) *the dynamic effect* where decreases in subsidence with warming (for a fixed inversion strength) results in an increase in the boundary layer thickness and thicker stratocumulus (assuming there is sufficient mixing within the boundary layer to maintain coupling between the cloud and surface), 3) *the thermodynamic effect* where a warmer sea-surface temperature or drier free troposphere results in a larger gradient in the specific humidity (across the inversion) that promotes more efficient turbulent entrainment-driven drying of the boundary layer and thins stratocumulus, and finally 4) *the stability effect* where a stronger inversion (larger EIS) results in less entrainment that lowers and thickens stratocumulus.

The radiative effect (which differ substantially between the solp4p and 4xCO2) is part of the adjustment to the solar and CO_2 forcing rather than the temperature mediated response, and so is discussed in detail in Part II which specifically addresses cloud adjustments (Aerenson et al., 2023). The other three mechanisms are nominally all present in the temperature mediated response. Mechanism 2 suggests that slowing circulations might result in an increase in stratocumulus with warming, while mechanisms 3 and 4 would decrease stratocumulus. As shown in **Figure 7** there is a reduction of subsidence with warming in stratocumulus regimes. However, no regions experience a net increase in low clouds, and so mechanism 2 is clearly not dominating the other response mechanisms. We note however, that a careful examination of **Figure 2** shows that there is an increase (purple colors) in optically medium mid-level, and to a lesser degree optically thick mid-level clouds (though we note there is poor model agreement). This is consistent with rising cloud tops in some models and mechanism 2 – *the dynamic effect* – is the only mechanism that causes rising stratocumulus cloud tops with warming. The remaining two mechanisms predict a decrease in cloudiness with increasing sea-surface temperature and EIS. There is low-cloud loss even in locations with decreasing EIS, which suggests that sea-surface temperature changes (*the thermodynamic effect*) likely play a dominant role in the changes of marine low-clouds. This result is consistent with the review paper by Klein et al. (2017) who find that sea-surface temperature is the leading cloud controlling factor for subtropical stratocumulus followed by EIS, and with lesser contributions from subsidence, advection, and free tropospheric relative humidity.

In the midlatitudes and subtropics outside of the stratocumulus regimes, low level clouds are commonly cumulus clouds, often called trade wind cumulus. Such trade cumulus also experiences substantial temperature mediated change; however they are often overlooked in favor of stratocumulus clouds, due stratocumulus clouds' tendency to dominate the low-cloud radiative effect and feedbacks. They can be understood through a similar framework of boundary layer moisture availability and free tropospheric drying as stratocumulus, and feedbacks from open-cell cumulus clouds have been found to be tightly linked with boundary layer convective mixing. (Sherwood et al., 2014; Vogel et al., 2022). We find a substantial decrease in low cloudiness in the warming experiments over Southern Hemisphere Ocean centered around 40° S that is larger (and more consistent between models) than that occurring in the Northern Hemisphere. Near this latitude in the Southern Hemisphere, there is relatively large sea-surface temperature increase (as compared with the global mean, or the Northern Hemisphere), a stronger temperature mediated decrease in EIS, and greater drying at 700 hPa, all of which may contribute to the decrease in low cloudiness. Zelinka et al. (2020) examined the cause of high cloud feedbacks in 4xCO2 between 60° and 30° S in CMIP5 and CMIP6 models. Through a multi-linear regression, they show that the decrease in low cloud amount in CMIP6 models is largely due to a combination of increasing EIS, and a drying of the free troposphere (reduction in 700 hPa relative humidity). The ensemble of models used by Zelinka et al. (2020) does include the models examined here, as such we expect the same mechanisms to be responsible.

Through the use of data produced in the EUREC^{4}A field campaign Vogel et al. (2022) find a near-zero trade-cumulus feedback (which disagrees with the feedback found here), they note that many models exaggerate the relationship between cloudiness and relative humidity.

Additionally, Vogel et al. (2022) show that models underestimate the coupling between clouds and mesoscale convection in trade cumulus regimes. Thus, the mechanisms controlling trade cumulus in our model simulations may not be the same as those which control trade cumulus on Earth.

Turning attention to the difference between the cloud response to 4xCO2 and solp4p, the largest difference occurs in the optically medium low cloud category, where there is about a 0.07% greater reduction of cloud with warming due to solar forcing than CO_2 forcing. This difference in low and mid-level cloud amount is consistent with a stronger *thermodynamic effect* in solp4p, as there is slightly greater warming in the tropics and subtropics in solp4p than occurs in the 4xCO2 (for an equivalent change in global mean temperature). The difference in warming pattern following solar and CO_2 forcing is further explored in Part II, which examines the cloud changes which are not mediated by global mean temperature change (including changing SST pattern effects). Zhou et al. (2023) find that warming patterns are a strong predictor of cloud feedbacks to a variety of forcing mechanisms such that a green's function approach can be used to reconstruct the feedback to a specific forcing agent if the warming pattern is known. In the solp4p experiment there is more warming in the tropics and subtropics than the 4xCO2 (shown in Part II), hence we speculate that the enhanced warming in the tropics of subtropics of solp4p (when compared with 4xCO2) causes a stronger cloud feedback via *the thermodynamic effect*.

In the cooling experiments, the positive feedback associated with oceanic low cloud increases (orange colors in **Figure 3**) is broadly similar, but somewhat weaker than in the warming experiments, and does not extend as far poleward. There is, however, a stronger (and more consistent) change in mid-level cloud over the Namibian, Australian, and Peruvian stratocumulus decks, associated with increases in subsident rates and consistent with a relatively strong *dynamic effect*.

4.3 <u>High Latitude Clouds</u>

In both warming experiments there is an increase in low and mid-level cloud optical depth poleward of about 60°, and the opposite response: a decrease in optical depth (poleward of about 40°) in both cooling experiments. This is evidenced in **Figures 2 and 3** as a reduction in optically thin clouds and an increase in optically medium and thick cloud in the warming experiments, and vice-versa in the cooling experiments.

As demonstrated by **Figure 10**, this change in optical depth (and its latitude) is collocated with a reduction in the relative fraction of condensate mass that is ice in the warming experiments (and increase in the cooling experiments). Cloud ice crystals tend to be larger than liquid droplets, and as such for an equivalent amount of condensate mass, there are more particles in a liquid cloud than an ice cloud and this causes ice clouds to be less reflective of sunlight than liquid clouds (e.g. Cesana & Storelvmo, 2017; Rogers & Yau, 1989). Additionally, for an equivalent liquid/ice water path liquid clouds are less efficient at precipitating, so liquid clouds tend to contain more water than ice clouds, which may cause them to be optically thicker and have longer lifetime (McCoy et al., 2015; Mitchell et al., 1989; Mülmenstädt et al., 2021; Senior & Mitchell, 1993; Tsushima et al., 2006). These theoretical expectations are supported by observations, including ground based measurements by Terai et al. (2019), who found that at high latitudes clouds with a mean temperature less than 0°C are observed to have an increased optical depth with warming.

The cloud changes shown in **Figures 2 and 3** are consistent with this expected cloud optical depth-phase feedback. Zhu & Poulsen (2020) likewise identified the latitude at which this cloud phase feedback occurs to shift and create a non-linearity in the amount of temperature change that occurs from different amounts of forcing. However, we note that the cloud optical depth changes seen in **Figures 2 and 3** might also be related to sea-ice changes (at least at very high latitudes), because shrinking sea-ice allows for greater heat absorption in the Summer and release in the Autumn, which deepens the boundary layer and thickens low clouds following Morrison et al. (2019).

4.4 Limitations of the Cloud Radiative Effect from Kernels

Using the cloud radiative kernels, we find that the previously mentioned cloud optical depth change associated with phase partitioning changes constitutes a positive feedback in the solm4p and 0p5xCO2, due to the increased reflectivity of the low-cloud layer, and relatively little feedback in the 4xCO2 and solp4p. This kernel-derived cloud feedback illustrates a limitation with the cloud radiative kernel method. The radiative kernels isolate the radiative effect of cloud changes from the effect of changes below the cloud layer which are often referred to as cloud masking effects (Zelinka et al., 2013). In the forced experiments we use cloud radiative kernels which correspond to the local surface albedo in the models' base-state. So, in the solp4p and 4xCO2 experiments, the cloud thickening does not cause a strong cloud feedback using the cloud radiative kernels because in the initial state, there is high-albedo sea-ice beneath the clouds, which diminishes the SW radiative effect of the clouds, and the kernel method does not account for the sea-ice reduction when calculating the radiative anomaly in the warmed climate, or the sea-ice growth in the cooled climate of solm4p and 0p5xCO2. In the **Supplemental Materials** the cloud radiative effect is calculated using a different method of taking the difference in the model top-of-atmosphere radiative flux changes calculated both with and without clouds included in the model's radiation calculation. While this method does not allow one to parse the change into those due to various cloud types, and only provides the total change due to clouds, it does include cloud masking effects. Using this method we find there is a positive cloud feedback over regions of sea-ice loss in the solp4p and 4xCO2, and a weaker cloud feedback over areas of sea-ice growth in solm4p and 0p5xCO2 than is found using the radiative kernel method, though this does not rise to a level that changes any of our discussion or conclusions.

5 Conclusions

We began this paper by posing the following two questions: 1) How do cloud feedbacks differ in response to abrupt changes in CO_2 and solar forcing? And 2) Are there symmetrical (equal and opposite) cloud feedbacks to an increase and a decrease of radiative forcing? Overall, this paper has allowed us to parse through the effects of solar and CO_2 forcing to determine what types of temperature mediated cloud changes occur from each forcing agent, and how temperature mediated cloud changes are different in warming and cooling model experiments of both CO_2 and solar forcing. In short, the answer to the first question is that the temperature mediated cloud feedbacks are quite similar between solp4p and 4xCO2, however there are small differences in the feedbacks (which we discuss further below). And concerning the second question we find numerous differences between the response to increase and decrease of radiative forcing, most notably are those related to cloud phase feedbacks and changes in tropical circulation.

Consistent with Kaur et al. (2023), we do see some differences in the surface warming pattern that results from differences in the pattern of radiative forcing between the solp4p and 4xCO2 forcing experiments. In particular, there is slightly greater warming in the tropics, and less warming near the poles in the solp4p experiment than in the 4xCO2 that we speculate is due to the radiative forcing in the solar experiment being larger in the tropics. This greater temperature increase in the tropics drives a greater loss in low-cloud amount in solp4p as compared with 4xCO2. This does not have a great impact on high cloud changes, because in both the solp4p and 4xCO2 the tropical high cloud changes are dominated by a weakening of the walker circulation, which causes cloud changes of similar magnitude in both the solp4p and 4xCO2.

Both Rose et al. (2014) and Salvi et al. (2022) found that forcing the midlatitudes causes more positive cloud feedbacks (yielding a less negative total feedback parameter) than CO_2 forcing, or forcing concentrated in the tropics. This relates to our study because CO_2 forcing is spatially uniform across the globe (due to the long lifetime of CO_2 making it evenly mixed through the atmosphere), and solar forcing is strongest in the tropics. In our comparison of cloud feedbacks from solar and CO_2 forcing, we find more positive feedbacks from solar than CO_2 forcing (**Figure 6**), which is opposite that suggested by Rose et al. (2014) and Salvi et al. (2022). The discrepancy of our findings may be due to numerous differences in our simulations, most notably that Rose et al. (2014) and Salvi et al. (2022) both forced the midlatitudes without also forcing the tropics. So their comparisons of midlatitude and tropical forcing with CO_2 forcing contained much larger differences in the geographical distribution of the forcing than our comparison of solar and CO_2 forcing. Such localized forcing may also create circulations and teleconnections that do not occur in our experiments. Hence, our results do not negate their conclusions, they do however show that the geographical differences between solar and CO_2 forcing are not sufficient to yield the feedback patterns found by Rose et al. (2014) and Salvi et al. (2022).

Regarding the question of how climate warming compares to climate cooling, our results are largely consistent with Chalmers et al., (2022), in that we find key differences between warming and cooling to occur at high latitudes, where the latitude at which ice processes are active in the pervasive low-level clouds and sea-ice extend farther equatorward from cooling. The greater spatial coverage of the cloud phase and sea-ice transition, as well as the increase in insolation with decreasing latitude causes the associated SW feedback to be stronger in the cooling experiments than warming experiments. This result is also consistent with work that has been done on non-linear feedbacks to different amounts of warming by Bloch-Johnson et al. (2021) and Zhu & Poulsen (2020), who also identified the sea-ice and cloud phase transitions as locations where of non-linear feedbacks are prominent.

The results of the solm4p and 0p5xCO2 experiments also indicate the importance of the temperature pattern in the tropics for dictating cloud feedbacks. We find that the zonal temperature gradient across the equatorial Pacific weakens from global warming far more than it strengthens due to global cooling, such that there is a stronger Walker circulation change as a response to warming than cooling. Chalmers et al., (2022) found a similar result by comparing simulations of 2xCO2 and 0p5xCO2 in CESM1. Our results with a multi-model ensemble (albeit a small one) solidify the robustness of the differences between warming and cooling found by Chalmers et al., (2022).

As a caution, we note this analysis was performed with a relatively small subset of the CMIP6 models, and although the results discussed are consistent across our set of models, they may not be representative of a larger ensemble. Additionally, we use single realizations from each model for each experiment, which limits our ability to assess whether differences between experiments surpass internal variability. We try to overcome such limitations by using model experiments with relatively large abrupt forcing, such that the signal to noise ratio is large, and derive temperature mediated cloud changes from relatively long model simulations (150 years), to dampen the importance of internal variability.

In closing, we have focused in this study on the temperature mediated component of could changes. We have found that differences between the temperature mediated response to solar and CO_2 radiative forcing are subtle, meaning the temperature mediated cloud changes are fairly insensitive to the forcing mechanism. This supports the underlying premise of the feedback model, that cloud feedbacks can be understood as a combination of the response to global temperature and an adjustment that occurs directly due to the forcing agent. If the abrupt changes in solar and CO_2 radiative forcing had resulted in a substantially differing temperature mediated cloud response, this would indicate that the temperature mediated component were not necessarily driven by global temperature, and instead were specific to the forcing agent. This is not to suggest that there are not differences in the responses, and we do find some driven by differences in the pattern of sea-surface temperature; only that these differences are modest on the 150 year time-scale examined here and given a similar total change in surface temperature. The magnitude of the forcing does matter, and indeed we found numerous differences between the cloud response to warming and cooling. Also, to be clear, there are larger differences in the cloud adjustment component of the response to solar and CO_2 forcing (meaning the cloud changes which are not mediated by global mean temperature), which is examined in detail in the companion paper to this (Part II Aerenson et al., 2023).

Acknowledgments

This research was supported by the MISR project at the NASA Jet Propulsion Laboratory (under contract no. 1318945). The authors wish to acknowledge and thank the many modelling centers who contributed data to the Coupled Model Intercomparison Project that was necessary for this study.

Open Research

All data used in this study are available for downlowad from the World Climate Research Program (WCRP) CMIP6 data archive (https://esgf-node.llnl.gov/search/cmip6/). Additionally the cloud radiative kernels were downloaded from https://github.com/mzelinka.

References

Adames, Á. F., & Wallace, J. M. (2017). On the tropical atmospheric signature of El Niño. *Journal of the Atmospheric Sciences*, *74*(6), 1923–1939. https://doi.org/10.1175/JAS-D-16-0309.1

Aerenson, T., Marchand, R., & Zhou, C (2023). Cloud Response to Abrupt Solar and CO_2 Forcing Part II: Adjustment to Forcing in Coupled Models *Journal of Geophysical Research: Atmospheres*, submitted

Aerenson, T., Marchand, R., Chepfer, H., & Medeiros, B. (2022). When Will MISR Detect Rising High Clouds? *Journal of Geophysical Research: Atmospheres*, *127*(2), e2021JD035865. https://doi.org/10.1029/2021JD035865

Andrews, T., & Ringer, M. A. (2014). Cloud feedbacks, rapid adjustments, and the forcing-response relationship in a transient CO2 reversibility scenario. *Journal of Climate*, *27*(4), 1799–1818. https://doi.org/10.1175/JCLI-D-13-00421.1

Armour, K. C., Bitz, C. M., & Roe, G. H. (2013). Time-Varying Climate Sensitivity from Regional Feedbacks. *Journal of Climate*, *26*(13), 4518–4534. https://doi.org/10.1175/JCLI-D-12-00544.1

Battisti, D. S., Vimont, D. J., & Kirtman, B. P. (2019). 100 years of progress in understanding the dynamics of coupled atmosphere–ocean variability. *Meteorological Monographs*, *59*(1), 8.1-8.57. https://doi.org/10.1175/AMSMONOGRAPHS-D-18-0025.1

Bjerknes, J. (1969). Atmospheric teleconnections from the equatorial Pacific. *Monthly Weather Review*, *97*(3), 163–172. https://doi.org/10.1175/1520-0493(1969)097<0163:atftep>2.3.co;2

Bjordal, J., Storelvmo, T., Alterskjær, K., & Carlsen, T. (2020). Equilibrium climate sensitivity above 5 °C plausible due to state-dependent cloud feedback. *Nature Geoscience*, *13*(11), 718–721. https://doi.org/10.1038/s41561-020-00649-1

Bloch-Johnson, J., Rugenstein, M., Stolpe, M. B., Rohrschneider, T., Zheng, Y., & Gregory, J.

M. (2021, February 28). Climate Sensitivity Increases Under Higher CO2 Levels Due to Feedback Temperature Dependence. *Geophysical Research Letters*, Vol. 48, p. e2020GL089074. https://doi.org/10.1029/2020GL089074

Bodas-Salcedo, A., Webb, M. J., Bony, S., Chepfer, H., Dufresne, J. L., Klein, S. A., … John, V. O. (2011). COSP: Satellite simulation software for model assessment. *Bulletin of the American Meteorological Society*, *92*(8), 1023–1043. https://doi.org/10.1175/2011BAMS2856.1

Boucher, O., Servonnat, J., Albright, A. L., Aumont, O., Balkanski, Y., Bastrikov, V., … Vuichard, N. (2020). Presentation and Evaluation of the IPSL-CM6A-LR Climate Model. *Journal of Advances in Modeling Earth Systems*, *12*(7), e2019MS002010. https://doi.org/10.1029/2019MS002010

Bretherton, C. S. (2015, November 13). Insights into low-latitude cloud feedbacks from high-resolution models. *Philosophical Transactions of the Royal Society A: Mathematical, Physical and Engineering Sciences*, Vol. 373. https://doi.org/10.1098/rsta.2014.0415

Byrne, M. P., & O'Gorman, P. A. (2013). Land-ocean warming contrast over a wide range of climates: Convective quasi-equilibrium theory and idealized simulations. *Journal of Climate*, *26*(12), 4000–4016. https://doi.org/10.1175/JCLI-D-12-00262.1

Ceppi, P., Brient, F., Zelinka, M. D., & Hartmann, D. L. (2017). Cloud feedback mechanisms and their representation in global climate models. *Wiley Interdisciplinary Reviews: Climate Change*, Vol. 8, p. 465. https://doi.org/10.1002/wcc.465

Cesana, G., & Storelvmo, T. (2017). Improving climate projections by understanding how cloud phase affects radiation. *Journal of Geophysical Research*, *122*(8), 4594–4599. https://doi.org/10.1002/2017JD026927

Chalmers, J., Kay, J. E., Middlemas, E. A., Maroon, E. A., & Dinezio, P. (2022). Does Disabling Cloud Radiative Feedbacks Change Spatial Patterns of Surface Greenhouse Warming and Cooling? *Journal of Climate*, *35*(6), 1787–1807. https://doi.org/10.1175/JCLI-D-21-0391.1

Chemke, R. (2022). Large hemispheric differences in the Hadley cell strength variability due to ocean coupling. *Npj Climate and Atmospheric Science*, *5*(1), 1–8. https://doi.org/10.1038/s41612-021-00225-3

Danabasoglu, G., Lamarque, J. F., Bacmeister, J., Bailey, D. A., DuVivier, A. K., Edwards, J., … Strand, W. G. (2020). The Community Earth System Model Version 2 (CESM2). *Journal of Advances in Modeling Earth Systems*, *12*(2), e2019MS001916. https://doi.org/10.1029/2019MS001916

Dufresne, J. L., & Bony, S. (2008). An assessment of the primary sources of spread of global warming estimates from coupled atmosphere-ocean models. *Journal of Climate*, *21*(19), 5135–5144. https://doi.org/10.1175/2008JCLI2239.1

Eyring, V., Bony, S., Meehl, G. A., Senior, C. A., Stevens, B., Stouffer, R. J., & Taylor, K. E. (2016). Overview of the Coupled Model Intercomparison Project Phase 6 (CMIP6) experimental design and organization. *Geoscientific Model Development*, *9*(5), 1937–1958. https://doi.org/10.5194/gmd-9-1937-2016

Frierson, D. M. W., Lu, J., & Chen, G. (2007). Width of the Hadley cell in simple and comprehensive general circulation models. *Geophysical Research Letters*, *34*(18), 18804. https://doi.org/10.1029/2007GL031115

Gregory, J. M., Ingram, W. J., Palmer, M. A., Jones, G. S., Stott, P. A., Thorpe, R. B., … Williams, K. D. (2004). A new method for diagnosing radiative forcing and climate sensitivity. *Geophysical Research Letters*, *31*(3). https://doi.org/10.1029/2003GL018747

Hartmann, D. L., & Larson, K. (2002). An important constraint on tropical cloud - climate feedback. *Geophysical Research Letters*, *29*(20), 12-1-12–14. https://doi.org/10.1029/2002gl015835

Held, I. M., & Soden, B. J. (2006). Robust responses of the hydrological cycle to global warming. *Journal of Climate*, *19*(21), 5686–5699. https://doi.org/10.1175/JCLI3990.1

Hulme, M. (2012). Climate change: Climate engineering through stratospheric aerosol injection. *Progress in Physical Geography: Earth and Environment*. https://doi.org/https://doi.org/10.1177/0309133312456414

Jeevanjee, N., & Fueglistaler, S. (2020). Simple spectral models for atmospheric radiative cooling. *Journal of the Atmospheric Sciences*, *77*(2), 479–497. https://doi.org/10.1175/JAS-D-18-0347.1

Joshi, M. M., Gregory, J. M., Webb, M. J., Sexton, D. M. H., & Johns, T. C. (2008). Mechanisms for the land/sea warming contrast exhibited by simulations of climate change. *Climate Dynamics*, *30*(5), 455–465. https://doi.org/10.1007/s00382-007-0306-1

Kaur, H., Bala, G., Seshadri, A. K., & Sciences, O. (2023). Why is Climate Sensitivity for Solar Forcing less than for an Equivalent. *Journal of Climate*, *36*(3), 1–39. https://doi.org/10.1175/JCLI-D-21-0980.1

Keith, D. W., Weisenstein, D. K., Dykema, J. A., & Keutsch, F. N. (2016). Stratospheric solar geoengineering without ozone loss. *Proceedings of the National Academy of Sciences of the United States of America*, *113*(52), 14910–14914. https://doi.org/10.1073/pnas.1615572113

Klein, S. A., Hall, A., Norris, J. R., & Pincus, R. (2017). Low-Cloud Feedbacks from Cloud-Controlling Factors: A Review. *Surveys in Geophysics*, *38*(6), 1307–1329. https://doi.org/10.1007/s10712-017-9433-3

Klein, S. A., & Hartmann, D. L. (1993). The seasonal cycle of low stratiform clouds. *Journal of Climate*, *6*(8), 1587–1606. https://doi.org/10.1175/1520-0442(1993)006<1587:TSCOLS>2.0.CO;2

Knutson, T. R., & Manabe, S. (1995). Time-mean response over the tropical Pacific to increased CO2 in a coupled ocean-atmosphere model. *Journal of Climate*, *8*(9), 2181–2199. https://doi.org/10.1175/1520-0442(1995)008<2181:TMROTT>2.0.CO;2

Lu, J., Vecchi, G. A., & Reichler, T. (2007). Expansion of the Hadley cell under global warming. *Geophysical Research Letters*, *34*(6), 6805. https://doi.org/10.1029/2006GL028443

McCoy, D. T., Hartmann, D. L., Zelinka, M. D., Ceppi, P., & Grosvenor, D. P. (2015). Mixed-phase cloud physics and Southern Ocean cloud feedback in climate models. *Journal of Geophysical Research*, *120*(18), 9539–9554. https://doi.org/10.1002/2015JD023603

Mitchell, J. F. B., Senior, C. A., & Ingram, W. J. (1989). CO2 and climate: A missing feedback? *Nature*, *341*(6238), 132–134. https://doi.org/10.1038/341132a0

Morrison, A. L., Kay, J. E., Frey, W. R., Chepfer, H., & Guzman, R. (2019). Cloud Response to Arctic Sea Ice Loss and Implications for Future Feedback in the CESM1 Climate Model. *Journal of Geophysical Research: Atmospheres*, *124*(2), 1003–1020. https://doi.org/10.1029/2018JD029142

Mülmenstädt, J., Salzmann, M., Kay, J. E., Zelinka, M. D., Ma, P. L., Nam, C., … Quaas, J. (2021). An underestimated negative cloud feedback from cloud lifetime changes. *Nature Climate Change*, *11*(6), 508–513. https://doi.org/10.1038/s41558-021-01038-1

Narsey, S., Brown, J. R., Delage, F., Boschat, G., Grose, M., Colman, R., & Power, S. (2022). Storylines of South Pacific Convergence Zone Changes in a Warmer World. *Journal of Climate*, *35*(20), 2949–2967. https://doi.org/10.1175/JCLI-D-21-0433.1

Niemeier, U., Schmidt, H., Alterskjær, K., & Kristjánsson, J. E. (2013). Solar irradiance reduction via climate engineering: Impact of different techniques on the energy balance and the hydrological cycle. *Journal of Geophysical Research Atmospheres*, *118*(21), 11,905-11,917. https://doi.org/10.1002/2013JD020445

Norris, J. R., Allen, R. J., Evan, A. T., Zelinka, M. D., O'Dell, C. W., & Klein, S. A. (2016). Evidence for climate change in the satellite cloud record. *Nature*, *536*(7614), 72–75. https://doi.org/10.1038/nature18273

Oort, A. H., & Yienger, J. J. (1996). Observed interannual variability in the Hadley circulation and its connection to ENSO. *Journal of Climate*, *9*(11), 2751–2767. https://doi.org/10.1175/1520-0442(1996)009<2751:OIVITH>2.0.CO;2

Qu, X., Hall, A., Klein, S. A., & Caldwell, P. M. (2014). On the spread of changes in marine low cloud cover in climate model simulations of the 21st century. *Climate Dynamics*, *42*(9–10), 2603–2626. https://doi.org/10.1007/s00382-013-1945-z

Qu, X., Hall, A., Klein, S. A., & Caldwell, P. M. (2015). The strength of the tropical inversion and its response to climate change in 18 CMIP5 models. *Climate Dynamics*, *45*(1–2), 375–396. https://doi.org/10.1007/s00382-014-2441-9

Roberts, M. J., Baker, A., Blockley, E. W., Calvert, D., Coward, A., Hewitt, H. T., … Luigi Vidale, P. (2019). Description of the resolution hierarchy of the global coupled HadGEM3-GC3.1 model as used in CMIP6 HighResMIP experiments. *Geoscientific Model Development*, *12*(12), 4999–5028. https://doi.org/10.5194/gmd-12-4999-2019

Rogers, R. R., & Yau, M. K. (1989). A short course in cloud physics. In *SERBIULA (sistema Librum 2.0)*. Retrieved from https://books.google.com/books?hl=en&lr=&id=ClKbCgAAQBAJ&oi=fnd&pg=PP1&ots=EnESDHWWHO&sig=0zuX8J8jMfiGoCtTgOgxPlkzGtE#v=onepage&q&f=false

Rose, B. E. J., Armour, K. C., Battisti, D. S., Feldl, N., & Koll, D. D. B. (2014). The dependence of transient climate sensitivity and radiative feedbacks on the spatial pattern of ocean heat uptake. *Geophysical Research Letters*, *41*(3), 1071–1078. https://doi.org/10.1002/2013GL058955

Salvi, P., Ceppi, P., & Gregory, J. M. (2022). Interpreting Differences in Radiative Feedbacks From Aerosols Versus Greenhouse Gases. *Geophysical Research Letters*, *49*(8), e2022GL097766. https://doi.org/10.1029/2022GL097766

Senior, C. A., & Mitchell, J. F. B. (1993). Carbon dioxide and climate: the impact of cloud parameterization. *Journal of Climate*, *6*(3), 393–418. https://doi.org/10.1175/1520-0442(1993)006<0393:CDACTI>2.0.CO;2

Shepard, J., Caldeira, K., Cox, P., Keith, D., Launder, B., Georgina, M., … Watson, A. (2009). *Geoengineering the climate: science, governance and uncertainty*. *Royal Soci*, 89.

Sherwood, S. C., Webb, M. J., Annan, J. D., Armour, K. C., Forster, P. M., Hargreaves, J. C., … Zelinka, M. D. (2020, December 25). An Assessment of Earth's Climate Sensitivity Using Multiple Lines of Evidence. *Reviews of Geophysics*, Vol. 58. https://doi.org/10.1029/2019RG000678

Sherwood, Steven C., Bony, S., & Dufresne, J. L. (2014). Spread in model climate sensitivity traced to atmospheric convective mixing. *Nature*, *505*(7481), 37–42. https://doi.org/10.1038/nature12829

Soden, B. J., & Held, I. M. (2006). An assessment of climate feedbacks in coupled ocean-atmosphere models. *Journal of Climate*, *19*(14), 3354–3360. https://doi.org/10.1175/JCLI3799.1

Staten, P. W., & Reichler, T. (2014). On the ratio between shifts in the eddy-driven jet and the Hadley cell edge. *Climate Dynamics*, *42*(5–6), 1229–1242. https://doi.org/10.1007/s00382-013-1905-7

Su, W., Bodas-Salcedo, A., Xu, K. M., & Charlock, T. P. (2010). Comparison of the tropical radiative flux and cloud radiative effect profiles in a climate model with Clouds and the Earth's Radiant Energy System (CERES) data. *Journal of Geophysical Research Atmospheres*, *115*(1), 1105. https://doi.org/10.1029/2009JD012490

Swart, N. C., Cole, J. N. S., Kharin, V. V., Lazare, M., Scinocca, J. F., Gillett, N. P., … Winter, B. (2019). The Canadian Earth System Model version 5 (CanESM5.0.3). *Geoscientific Model Development*, *12*(11), 4823–4873. https://doi.org/10.5194/gmd-12-4823-2019

Taylor, K. E., Crucifix, M., Braconnot, P., Hewitt, C. D., Doutriaux, C., Broccoli, A. J., … Webb, M. J. (2007). Estimating shortwave radiative forcing and response in climate models. *Journal of Climate*, *20*(11), 2530–2543. https://doi.org/10.1175/JCLI4143.1

Terai, C. R., Zhang, Y., Klein, S. A., Zelinka, M. D., Chiu, J. C., & Min, Q. (2019). Mechanisms Behind the Extratropical Stratiform Low-Cloud Optical Depth Response to Temperature in ARM Site Observations. *Journal of Geophysical Research: Atmospheres*, *124*(4), 2127–2147. https://doi.org/10.1029/2018JD029359

Tsushima, Y., Emori, S., Ogura, T., Kimoto, M., Webb, M. J., Williams, K. D., … Andronova, N. (2006). Importance of the mixed-phase cloud distribution in the control climate for assessing the response of clouds to carbon dioxide increase: A multi-model study. *Climate Dynamics*, *27*(2–3), 113–126. https://doi.org/10.1007/s00382-006-0127-7

Vogel, R., Albright, A. L., Vial, J., George, G., Stevens, B., & Bony, S. (2022). Strong cloud–

circulation coupling explains weak trade cumulus feedback. *Nature*, *612*(7941), 696–700. https://doi.org/10.1038/s41586-022-05364-y

Webb, M. J., Andrews, T., Bodas-Salcedo, A., Bony, S., Bretherton, C. S., Chadwick, R., … Watanabe, M. (2017). The Cloud Feedback Model Intercomparison Project (CFMIP) contribution to CMIP6. *Geoscientific Model Development*, *10*(1), 359–384. https://doi.org/10.5194/gmd-10-359-2017

Williams, A. I. L., Jeevanjee, N., & Bloch-Johnson, J. (2023). Circus Tents, Convective Thresholds, and the Non-Linear Climate Response to Tropical SSTs. *Geophysical Research Letters*, *50*(6), e2022GL101499. https://doi.org/10.1029/2022GL101499

Williams, K. D., Ingram, W. J., & Gregory, J. M. (2008). Time variation of effective climate sensitivity in GCMs. *Journal of Climate*, *21*(19), 5076–5090. https://doi.org/10.1175/2008JCLI2371.1

Wood, R. (2012, August 1). Stratocumulus clouds. *Monthly Weather Review*, Vol. 140, pp. 2373–2423. https://doi.org/10.1175/MWR-D-11-00121.1

Wood, R., & Bretherton, C. S. (2006). On the relationship between stratiform low cloud cover and lower-tropospheric stability. *Journal of Climate*, *19*(24), 6425–6432. https://doi.org/10.1175/JCLI3988.1

Yukimoto, S., Kawai, H., Koshiro, T., Oshima, N., Yoshida, K., Urakawa, S., … Ishii, M. (2019). The meteorological research institute Earth system model version 2.0, MRI-ESM2.0: Description and basic evaluation of the physical component. *Journal of the Meteorological Society of Japan*, *97*(5), 931–965. https://doi.org/10.2151/jmsj.2019-051

Zelinka, M. D., & Hartmann, D. L. (2010). Why is longwave cloud feedback positive? *Journal of Geophysical Research Atmospheres*, *115*(16). https://doi.org/10.1029/2010JD013817

Zelinka, M. D., Klein, S. A., & Hartmann, D. L. (2012a). Computing and partitioning cloud feedbacks using cloud property histograms. Part I: Cloud radiative kernels. *Journal of Climate*, *25*(11), 3715–3735. https://doi.org/10.1175/JCLI-D-11-00248.1

Zelinka, M. D., Klein, S. A., & Hartmann, D. L. (2012b). Computing and partitioning cloud feedbacks using cloud property histograms. Part II: Attribution to changes in cloud amount, altitude, and optical depth. *Journal of Climate*, *25*(11), 3736–3754. https://doi.org/10.1175/JCLI-D-11-00249.1

Zelinka, M. D., Klein, S. A., Taylor, K. E., Andrews, T., Webb, M. J., Gregory, J. M., & Forster, P. M. (2013). Contributions of different cloud types to feedbacks and rapid adjustments in CMIP5. *Journal of Climate*, *26*(14), 5007–5027. https://doi.org/10.1175/JCLI-D-12-00555.1

Zelinka, M. D., Myers, T. A., McCoy, D. T., Po-Chedley, S., Caldwell, P. M., Ceppi, P., … Taylor, K. E. (2020). Causes of Higher Climate Sensitivity in CMIP6 Models. *Geophysical Research Letters*, *47*(1). https://doi.org/10.1029/2019GL085782

Zhu, J., & Poulsen, C. J. (2020). On the Increase of Climate Sensitivity and Cloud Feedback With Warming in the Community Atmosphere Models. *Geophysical Research Letters*, *47*(18), e2020GL089143. https://doi.org/10.1029/2020GL089143